Gas Core Reactor Numerical Simulation Using a Coupled MHD-MCNP Model

F. Kazeminezhad
Institute for Scientific Research, Inc., Faimont, West Virginia

S. Anghaie
University of Florida, Gainesville, Florida

The NASA STI Program…in Profile

Since its founding, NASA has been dedicated to the advancement of aeronautics and space science. The NASA Scientific and Technical Information (STI) Program Office plays a key part in helping NASA maintain this important role.

The NASA STI program operates under the auspices of the Agency Chief Information Officer. It collects, organizes, provides for archiving, and disseminates NASA's STI. The NASA STI program provides access to the NASA Aeronautics and Space Database and its public interface, the NASA Technical Report Server, thus providing one of the largest collections of aeronautical and space science STI in the world. Results are published in both non-NASA channels and by NASA in the NASA STI Report Series, which includes the following report types:

- TECHNICAL PUBLICATION. Reports of completed research or a major significant phase of research that present the results of NASA programs and include extensive data or theoretical analysis. Includes compilations of significant scientific and technical data and information deemed to be of continuing reference value. NASA's counterpart of peer-reviewed formal professional papers but has less stringent limitations on manuscript length and extent of graphic presentations.

- TECHNICAL MEMORANDUM. Scientific and technical findings that are preliminary or of specialized interest, e.g., quick release reports, working papers, and bibliographies that contain minimal annotation. Does not contain extensive analysis.

- CONTRACTOR REPORT. Scientific and technical findings by NASA-sponsored contractors and grantees.

- CONFERENCE PUBLICATION. Collected papers from scientific and technical conferences, symposia, seminars, or other meetings sponsored or cosponsored by NASA.

- SPECIAL PUBLICATION. Scientific, technical, or historical information from NASA programs, projects, and missions, often concerned with subjects having substantial public interest.

- TECHNICAL TRANSLATION. English-language translations of foreign scientific and technical material pertinent to NASA's mission.

Specialized services also include creating custom thesauri, building customized databases, and organizing and publishing research results.

For more information about the NASA STI program, see the following:

- Access the NASA STI program home page at <http://www.sti.nasa.gov>

- E-mail your question via the Internet to <help@sti.nasa.gov>

- Fax your question to the NASA STI Help Desk at 301– 621–0134

- Phone the NASA STI Help Desk at 301– 621–0390

- Write to:
  NASA STI Help Desk
  NASA Center for AeroSpace Information
  7115 Standard Drive
  Hanover, MD 21076–1320

Gas Core Reactor Numerical Simulation Using a Coupled MHD-MCNP Model

F. Kazeminezhad
Institute for Scientific Research, Inc., Faimont, West Virginia

S. Anghaie
University of Florida, Gainesville, Florida

May 2008

Acknowledgments

TABLE OF CONTENTS

TABLE OF CONTENTS (Continued)

LIST OF FIGURES

LIST OF TABLES

1 ABSTRACT

We suggest using two head-on magnetohydrodynamic (MHD) shocks to achieve supercritical nuclear fission in an axially elongated cylinder filled with UF_4 gas as an energy source for deep space missions. The motivation for each aspect of the design is explained and supported by theory and numerical simulations in this report. A subsequent report will provide detail on relevant experimental work to validate the concept.

In this report we focus on the theory of and simulations for the proposed gas core reactor conceptual design from the onset of shock generations to the supercritical state achieved when the shocks collide. To model the shock generation and propagation, an MHD code developed by one of the authors at ISR is primarily used. The MHD model is coupled to a standard nuclear code (MCNP), primarily by the authors at the University of Florida, Institute for Nuclear Space Power and Propulsion Institute, to observe the neutron flux and fission power attributed to the supercritical state brought about by the shock collisions. Throughout the modeling, realistic parameters are used for the initial ambient gaseous state and currents to ensure a resulting super-critical state upon shock collisions.

In some trials, power densities of 10^{10} MeV.cm^{-3} are seen at the time of maximum density, and this can grow to 10^{30} MeV.cm^{-3} or even greater if the gas is left unperturbed in the center of the shock tube. This is a novel effect that was not predicted and has not been fully evaluated as a possible means of fission power conversion; the cycle time should be on the order of a few milliseconds.

2   NUMERICAL SIMULATION COUPLED MHD-MCNP CODES

The broad aim of this research is to present methodologies and simulation results from research conducted into the modeling of shock wave driven gas core reactor systems. The initial concept under investigation could be described as a pulsed magnetic induction gas core reactor (PMI-GCR). The idea is that a strong ionizing set of twin shock waves would be generated in a fissile fuel filled shock tube, and that these shocks would then collide in the vicinity of a neutron moderator material providing a brief explosive burst of fission energy further ionizing the gas fuel and creating outgoing shock waves strong enough to allow an effect magneto-cumulative flux-compression generator (MCFG) system in pick-up solenoid coils, thus extracting pulsed electrical power. This energy extraction mechanism is the origin of the "PMI" in PMI-GCR. The reactor side of this system however is the primary component of interest in this report. Thus although the entire system involves three coupled stages, (1) shock generation, (2) shock interaction and fission energy release, (3) MCFG power extraction, the scope of this report extends only to the fission energy release stage with minor comments on the shock generation stage. The specific aim of this report is to document various simulation approaches to modeling the generation of the colliding shock waves and to present preliminary results showing the fission power energy generated as the two incoming shock waves collide. Power conversion (item (3)) is not included in this report, although previous reports have discussed the principle including Phase-I reports on this project.

Unlike most pulsed high magnetic field research the present concept under investigation does not use destructive explosives and is intended to by a fully functioning power cycle design. Although the release of fission energy in a short burst, sufficient for net power production, seems likely to require destructive energies this need not be the case as the results of this report show. Indeed, with the disk-like geometry of two colliding gas shocks it is rather astounding that fission criticality can be achieved at all. The system is therefore quite safe, at least in that it requires a great deal of effort to produce supercritical conditions. The goal however is to demonstrate extreme shock-wave pile-up in order to demonstrate prompt criticality and useful energy release. To perform this feat in a power cycle is a tremendous challenge and may place demands upon materials that go beyond the current state of the art in shock tube technology and vessel integrity. The investigation of such materials issues and feasibility of cyclical operation of a putative PMI-GCR system is however beyond the scope of this report. This report investigates only the shock generation and fission power release on the assumption that materials will exist that can withstand many repeated firings of such a system.

This report summarizes recent work on developing modeling tools for simulating the pulsed magnetic induction (shock wave driven) gas core reactor concept (PMI-GCR). The goal of modeling the shock generation and fission power production for this type of shock-wave driven gas core reactor is a complicated task for many reasons. For one, there is no general-purpose code for coupled solutions of gas dynamic equations and neutron transport equations. Although such a code could be developed the software development time would be excessive. Earlier proposals sought ambitiously to model the entire system from shock generation to magnetic flux compression power extraction. Owing to difficulties in obtaining adequate general purpose nuclear and magneto-gas dynamic codes the current proposal is scaled back to just simulating shock generation and fission power production in the shock-tube reactor. Another difficulty concerns the highly nonlinear MHD shock evolution and interaction. For this reason a 1-dimensional MHD code has been used and coupled to the Monte Carlo N-Particle (MCNP) code from LANL. In future work this will have to be replaced by 2D and eventually 3D MHD codes to estimate accurately the losses in the system, but for now the requirement of a working model to investigate various operational regimes and scaling principles for the PMI-GCR concept has required that these real effects be suppressed.

This report then describes how the 1D MHD code has been coupled with MCNP to yield a simulation tool suitable for exploring the ideal characteristics of a PMI-GCR system from shock generation initiation to fission energy release. The power extraction part of the cycle has not yet been implemented and requires solving difficult plasma kinetic problems as well as collection of preliminary experimental data on UF4 plasma characteristics before any realistic estimates of the system efficiency and specific power can be obtained.

A Linux platform was chosen for compiling the codes, as it was felt that parallelization of the codes may be desired later. The available MHD code was written in Fortran, but input/output handling is easier to coordinate with C/C++ routines and Linux scripts. So a multiple code mentality was used, where separate executables would be run and coordinated by a script program. Although it is possible for a Fortran program to call a C/C++ program, and vise versa, it is easier to either write a single code so that data is accessible globally, or to write a script that runs separate executables. We choose the scripting approach. In this way the compilation of the executables is easier to manage because they are independent of each other.

This report also includes partial documentation for the code 'mhd1dshock' used in ISR (Institute for Scientific Research (Fairmont, WV) and INSPI (Innovative Nuclear Space Power and Propulsion Institute, University of Florida) research into UF4-fuelled shock wave driven gas core nuclear reactors. The complete code uses a Linux script to batch process two main programs, 'mhd1dshock' and 'MCNP4C'. The first, 'mhd1dshock' is a magneto-gas dynamic code that uses flux corrected transport (FCT) to solve the MHD governing equations, while MCNP is a Monte Carlo transport code used in the combined ISR-INSPI code to obtain nuclear data for input into the MHD code. The MHD code used is a "1½"-dimensional code which solves the initial-BVP equations for the variables (ρ, v_x, v_y, p, B_y). This is suitable for shock tube geometries where azimuthal symmetry holds; the axial magnetic field B_x is constant. This enables qualitative scoping calculations for a shock wave driven gas core nuclear reactor design to be rapidly developed with a minimum of complication so that crucial experiments can be suggested. Once the physics of the 1-dimensional case are known and rough regimes determined for viable reactor operation (length scales, pressures, scalar gas conductivity, boundary conditions, and other dominant parameters) then full-blown 2 or 3D code can be deployed. This may be documented at a later stage of R&D, probably most feasibly only after some preliminary experimental data is gathered to support the preliminary modeling in this report.

Sections 4, 5 and 6 are basically devoted to the theory of current driven shock waves and how they impact the conceptual design. For Section 6 of the report we review the conceptual design of a few possible PMI-GCR variations, where the PMI-GCR concept is regarded as a class in the wider category of ambient-sub critical pulsed reactor types. Section 7 of the report considers the task of coupling the MHD code to the general purpose Monte Carlo neutron transport code MCNP4C that was used to calculate fission power source terms and neutron flux in the shock tube and surrounding BeO moderator material. Subsections 7.1 to 7.4 describe the MHD model and deal with modifications to the MHD code to allow communication with MCNP. Subsection 7.7 describes the nuclear-MCNP modeling aspects of this project.

After describing the coupling of the two codes simulation results are discussed in Section 8. Section 9 then discusses prospects for future research on the concept design for the PMI-GCR along with a final report summary for this phase of research on the power production leg of the system.

4

3   CURRENT DRIVEN SHOCK WAVES

Several mechanisms were considered suitable for achieving localized ionization, acceleration as well as heating of the ambient gas in ways which minimize the damage to the boundaries, current driven shocks appeared most promising, because they fulfill the following conditions:

3.1   *Boundary Generated*

Shocks get triggered by the application of current at the boundary of the proposed reactor core. To be more precise, the so-called step function currents are used; these are localized currents with infinitely short rise times (or short compared with the characteristic time scales with a corresponding short spatial scale). Their highly localized nature will trigger localized gradients in hydrodynamic as well as electromagnetic parameters suitable in triggering shocks as well as exciting MHD fast wave modes, which can steepen to form shocks.

3.2   *Ionize the Ambient Gas*

The boundary-generated currents advect into the device along with other accompanying hydrodynamic variables. The electric field associated with the current can ionize the ambient UF4 gas as the shock travels into the medium. This is in addition to the shock heating ionization that can take place if the incoming wave steepens to suitably high amplitude. However localized ionization by currents will be most effective against high recombination rate in a problem of localized nature.

3.3   *End Wall Damage Minimized*

The use of currents as opposed to moving mechanical parts in generating shock waves insures minimum damage to the mechanical boundary; e.g., erosion, fatigue and interaction of nuclear material with the walls are potentially very serious issues for the boundary material, which should be minimized.

3.4   *Wave Steepening Capability*

Most hydro or even MHD shocks arise from discontinuities. As such in the shock frame steady state conditions apply, or in the lab frame a shock leaves a uniform state behind it. Such a uniform state possesses global characteristics and will not be suitable for applications in which localized states with given hydrodynamic conditions are desired; e.g. conditions required for super-criticality. Only shock waves that arise from wave steepening can yield such characteristics, are time dependent, and therefore are not steady state solutions of the MHD or fluid equations. Current driven shocks can be used to form wave steepening.

3.5   *Why Two Shocks*

Two shocks are proposed as a means to enhance the steepening process. Consequently one could obtain from the two colliding shocks, one state that has density, pressure not a

linear sum of the incoming shocks. The advantage of this process is that one can achieve much higher densities and pressures at considerably smaller shock tube lengths. This will be most useful when dealing with applications that have serious constraints for the length of the device one intends to use.

4 SHOCK GENERATION MECHANISM

The device we propose to use relies on the application of a step function radial current at the boundary of a cylindrical device. Fundamentally we propose a design similar to that suggested by Patrick (1959)[1], Cloupeau (1963)[2], Kholev and Poltavchenko (1960)[3] for shock studies, and more recently used for another application in plasma focusing by Moreno et al (2003)[4]. The device relies on generating a radial step function current by capacitor discharge. Depending on whether one uses a pulsed versus a steady boundary current, one has the option of triggering either a discontinuity driven or wave steepened shock, or a combination of both. In the applications above, however, the authors primarily used pulsed currents.

To generate two shocks, radial currents are applied at the two ends. Each radial current Jr is associated with an azimuthal magnetic field Baz. Thus they result in a force $Jr \otimes Baz$ on the fluid on each end. The currents can be applied so that the force can be directed into the box at each end. Fig. 1 represents a schematic representation of the current-driven double shocks. If there exists an axial component of the magnetic field, the current Jr and its accompanying Baz will get transported into the cylinder; this is the so-called switch on fast shock.

[1] Patrick, Physics of fluids, 2, 589, (1959).
[2] Cloupeau, Physics of Fluids, 6, 679, (1963).
[3] Kholev and Poltavchenko, Doklady Akad. Nauk SSSR, Vol. 131, No. 5, pp. 1060-1063, April, 1960.
[4] Moreno, Casanova, Corea and Clausse, Plasma phys. Control Fusion 45 (2003).

Figure 1. Schematic representation of the double shock generation at the boundaries using radial currents with their accompanying azimuthal magnetic fields.

5   ANALYTIC MODEL

For an elongated device as shown above, one can safely assume major spatial variations to take place along the axial direction. However, given the vital role played by the radial current and its accompanying azimuthal magnetic field and their advection into the device with the shock, the model should account for the variations of Baz and its accompanying flow velocity. As such a 1.5 dimensional MHD model is most appropriate.

5.1   *MHD Model Equations*

We designate the axial direction to be **x** and the azimuthal direction **y**. The relevant MHD equations of continuity, momentum, energy and Faraday's law are, respectively:

$$\partial \rho / \partial t + \partial / \partial x (\rho V_x) = 0$$

$$\partial (\rho V_x) / \partial t + \partial / \partial x [\rho V_x^2 + P + 1/2(B_y^2 - B_x^2)] = 0$$

$$\partial (\rho V_y) / \partial t + \partial / \partial x [\rho V_y V_x - B_y B_x] = 0$$

$$\partial / \partial t [1/2 \rho (V_x^2 + V_y^2) + P/(\gamma - 1) + 1/2(B_x^2 + B_y^2)] +$$

$$\partial / \partial x [\rho V_x (1/2(V_x^2 + V_y^2) + \gamma P/(\gamma - 1)\rho) + V_x B_y^2 - V_y B_x B_y] = 0$$

$$\partial B_y / \partial t + \partial / \partial x [V_x B_y - V_y B_x] = 0$$

$$\partial B_x / \partial x = 0$$

5.2   *The Geometry of the Model*

Fig. 1 shows the general field and current configurations in the model; Fig. 2 depicts the geometry used in obtaining the analytic as well as numerical solutions to the 1.5 dimensional MHD equations above.

7

Figure 2. The field and current geometry used in the model. These represent the applied currents and their accompanying fields at the two ends of the proposed device.

Here the applied boundary currents (Jz) at the two ends of the box trigger shock waves into the conceptual device by their respective forces ($J_z \times B_y$) forces.

5.3 *Analytic Solutions*

A shock can get triggered for each of the applied currents above. The most important characteristic of such a shock is the presence of the transverse component of the magnetic field as it travels into the conceptual device. Such shocks are labeled as switch on shocks and have been observed in both laboratory and space physical plasmas. In this section we will derive the conditions under which such shocks can get triggered. Although ultimately the method used to generate the shocks in the simulations will be different, they are based on the switch on shock concept. The switch-on shock, though in its simplest form results from the application of a single step function current pulse, has exact analytic solution. That can provide useful insights into the simulation results, which will follow.

The switch on shock solutions are obtained using discontinuity theory. Using the standard wave frame calculations, as in Kemp and Petschek [5] and Bazer[6], one will obtain the following solutions to the above MHD equations after applying the current and field discontinuities above as follows:

$$V_{x_2}^{\ 2} = B_x^{\ 2} / \rho_2 = b_{x_1}^{\ 2}$$

$$(\rho_1 V_{x_1} / 2)(\gamma + 1)/(\gamma - 1)V_{x_2}^{\ 2} + [-\gamma/(\gamma - 1)(\rho_1 V_{x_1}^{\ 2} + P_1 - B_{y_2}^{\ 2}/2) - B_{y_2}^{\ 2}]V_{x_2}$$

$$+1/2\rho_1 V_{x_1}^{\ 3} + \gamma/(\gamma - 1)P_1 V_{x_1} + 1/2B_x^{\ 2}B_{y_2}^{\ 2}/(\rho_1 V_{x_1}) = 0$$

$$V_{y_2} = B_x /(\rho_1 V_{x_1})B_{y_2}$$

[5] Kemp and Petschek, Physics of fluids, 2, 599, (1959).
[6] Bazer, Astrophys. J. 128, 686, (1958).

8

where the subscripts 1 and 2 refer to the un-shocked and shocked regions respectively. Clearly $B_{y_1} = 0$, and $B_{x_1} = B_{x_2}$ from the last equation above. Using V_{x_2} and V_{y_2} of the first and the third equations into the second equation gives the following relationship for the switch on field component:

$$B_{y_2}^2 / B_x^2 = 2(\rho_2 / \rho_1 - 1)\{1 - .5(\gamma - 1)(\rho_2 / \rho_1 - 1) - \gamma P_1 / B_x^2\} \ .$$

This equation furnishes both the condition of the onset as well as some important implications of the switch on shock; i.e., for the right hand side to be positive we must have:

(a) $\rho_2 / \rho_1 \geq 1$, which also implies that $V_{x_1}^2 / b_{x_1}^2 \geq 1$;

this is consistent with steepening. Furthermore, since $V_{x_1} \geq b_{x_1}$ (the Alfven speed in the upstream un-shocked region) then this shock is a fast shock. Since the flow velocity downstream V_{x_2} is simply Alfven speed, this shock must also be an intermediate shock.

The second condition that results from the above is:

(b) $\rho_2 / \rho_1 = V_{x_1}^2 / b_{x_1}^2 \leq (\gamma + 1)(M_1^2 / 2)[(\gamma - 1)M_1^2 / 2 + 1]$;

where $M_1^2 = V_{x_1}^2 / (\gamma P_1 / \rho_1)$ is the Mach number in the un-shocked region. This relationship's right hand side is simply ρ_2 / ρ_1 of a pure hydro shock. Therefore, as expected for the MHD shock, the density steepening is lower than its corresponding hydro shock because some of the shock energy goes into the magnetic field steepening. However, as will be seen in the simulation section for the double shock simulations, heating can be substantially higher in this case, compared to the hydro case, if the magnetic energy that goes into the MHD shock can be turned into thermal energy by shock collisions.

The equation above for $B_{y_2}^2 / B_x^2$ suggests shock generation by perturbation of only one parameter, B_{y_2}. Most discontinuity generated shocks demand perturbation in all the independent parameters. This property has far reaching implications: it simplifies shock generation, it enables calculation of all the downstream parameters in terms of one, and can be used to trigger non steady state and time dependent downstream states.

The B_{y_2} / B_x equation suggests at least two means to manipulate downstream parameters: (a) by application of very large currents with the resulting downstream parameters of desired size, or (b) by holding a relatively small current steady for a finite length of time. Case (a) corresponds to a pulsed current case, while case (b), which will demand maintaining open boundaries while the current is on, resembles the mechanism of a thruster into the conceptual tube at each end. From this point on we will refer to the two cases as the pulsed versus magnetoplasma dynamics (MPD) thrusters respectively.

In the former case, the size of ρ_2 and consequently V_{x_1} and V_{x_2} are completely determined by B_{y_2} and since the boundary closes as the current is turned off, instead of a discontinuity with upstream and downstream states possessing global characteristics, a single pulse results (with front speed V_{x_1}) followed by a rarefaction wave. In the latter case, the continuous current pulse can be thought to result from infinitely many short duration pulses. There each pulse enters a denser medium perturbed by its predecessor with larger speed. It can, therefore, take over and merge the predecessor and give rise to a larger pulse. In both cases the impact is time dependent, strongly governed by the steepening process.

We shall next present the numerical simulation results of the MHD code as well as the MHD-MCNP coupled codes modeling a conceptual reactor from the shock generation to the fission triggering.

6   PMI-GCR CONCEPTUAL DESIGN OVERVIEW

Generally for the shock generation a coaxial arrangement of anode and cathode as depicted in Fig. 3 can be used. Such a design ensures very strong self field (B_θ) accompanying a strong radial current J and therefore strong pondromotive ($J \times B_\theta$) force. The strong radial current J serves to ionize the gas too.

Where the radial current ends the field of the solenoid begins which can trigger the switch-on shock and allow advection of both J and B_θ into the device. Application of two such currents (with mirror symmetry) at the two ends of a coaxial cylindrical device will result in head-on shocks.

Although many variations on the same theme could be generated, this report is concerned only with two specific classes of pulsed magnetic field shock-driven reactors. One is termed an "MPD compressor mode" device; the other is a "pulsed high magnetic field" device. The distinction between the two types is the method of shock wave generation at each end of the shock tube reactor. In practice the distinction between these two shock generation methods ("compressor-type" and "pulsed-type") becomes blurred and indistinguishable when the pulse time is set fairly large and the current density at the boundary is reduced: in that case, a pulse becomes almost indistinguishable from a short-duration MPD-compressor mode. The reason a sharp distinction cannot always be made is because, to operate in a pulsed high B-field mode, the gas fuel has to be highly ionized, and this generally requires a large current discharge through the gas. Consequently ponderomotive force effects will play a dominant role in addition to the desired magnetic discontinuity shock inducing effect. Thus, for high B-fields, shock waves will be created in the gas through two effects, one through the ponderomotive force and the other via magnetic and the resulting pressure discontinuity. These two effects may compete or cooperate depending upon the design of the shock generator, its geometry and electrode configuration.

The term "MPD compressor mode" is used because for smaller current densities and longer pulse duration times, the shock generation arises mainly from nonlinear wave steepening as described in the analytic section above and Wu [7]. For short pulse times and large current densities the shock generation can be said to arise more from steep magnetic pressure gradient at the boundaries giving rise to shocks from the feedback of magnetic pressure discontinuity into the gas through classical magneto-gas dynamic coupling, as described in Knoepfel[8]. There is, however, a regime where a true pulsed mode could be identified as distinct from a compressor mode by examining the time scales for collisional, relaxation and ionization processes; such an analysis should reveal when the transition from discontinuity-induced to pondermotive force-induced shock occurs. This report did not look closely at these issues however; since we believe that both mechanisms are at work, but with pondromotive to dominate the former. In both cases the coaxial setup depicted can be used with simple change in the duration of the applied currents and UF4 gas injection.
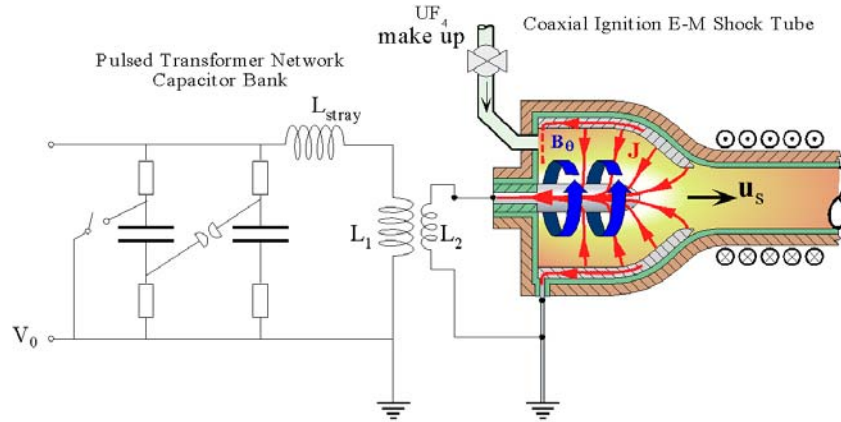
Figure 3. Representative generic coaxial or annular electromagnetic-driven shock tube.

The inner electrode here can be extended the entire length of the tube if a steady state annular shock wave is desired. This is probably unsuitable for the PMI-GCR system, however if the electrode was extended only part-way into the shock tube an annular tube geometry could be maintained by making the central tube ut of some moderator material perhaps even mixed with a small fraction of solid fissile fuel .

[7] C.C. Wu, "Formation, Structure, and Stability of MHD Intermediate Shocks", *J. Geophysical Research*, **95**, No.A6, 8149-81475, 1990.

[8] H.Knoepfel, "Pulsed High Magnetic Fields", North-Holland, 1970, in particular chapters 6 to 8.

7   SHOCK GENERATION AND INTERACTION MODEL

The overall viability of the PMI-GCR concept depends upon three crucial subcomponents: (1) the efficiency and efficacy of generating strong shock waves in the comparatively large diameter, high pressure shock tube, (2) design of the core interaction region for release of fission energy, and (3) magneto-cumulative flux-compression power extraction. This section discusses the first of these components.

7.1   *MHD Equations for Electromagnetic Shock Tube*

The governing equations of weak MHD can be derived by adding electromagnetic source terms to the Navier-Stokes equations. The continuity equation is unchanged because the mass density of the electromagnetic field is negligible. We can write mass conservation in the following form,

$$\frac{\partial \rho}{\partial t} + \nabla \cdot (\rho \mathbf{v}) = 0$$

Here ρ is the fluid density, and v the velocity, so $\rho \mathbf{v}$ is the momentum per unit volume of fluid. The momentum equation is a vector equation for $\rho \mathbf{v}$. If we apply Newton's 2nd law to a control volume, with external forces per unit volume $\mathbf{F}^{ext}$, and pressure-stress tensor $\mathbb{T}$, and then apply Gauss' law to reduce the integral equations to differential form, then momentum conservation takes the form,

$$\frac{\partial}{\partial t}(\rho \mathbf{v}) + \nabla \cdot (\rho \mathbf{v}\mathbf{v}) = \mathsf{F}^{\,ext} + \nabla \cdot \mathbf{T}$$

In this research the only body force is taken to be the ponderomotive force per unit mass, $\mathbf{F}^{em}$, which is derived from the Lorenz force. The Lorenz force law on moving charges together with the charge conservation law imply that the external body force is therefore,

$$\mathsf{F}^{\,em} = \rho^{(c)}\mathbf{E} + \frac{1}{c}\mathbf{J} \times \mathbf{B}$$

here $\rho^{(c)}$ is the charge density, and $\mathbf{E}$, $\mathbf{B}$ and $\mathbf{J}$ are the fields and total current density respectively in *the stationary observer frame* that sees the fluid moving at velocity $\mathbf{v}$. For overall neutral gases one can safely assume $\rho^{(c)}=0$ over even small volume elements. The choice of units here is Gaussian (cgs), for which $\mu_0 = \varepsilon_0 \approx 1$. We also make the usual MHD approximations (scalar conductivity, negligible Hall term in Ohm's law), for which Ohm's law reduces to,

$$\mathbf{J} = \sigma\mathbf{E} + \frac{1}{c}\mathbf{v} \times \mathbf{B} \, ,$$

so that σ is the scalar electrical conductivity of the fluid.

12

An energy equation for MHD can be derived easily by assuming a linear isotropic fluid, and then balancing (right-hand side say=) the *rate of increase of total energy with the sum of* (1) work done by surface stresses, (2) work done by external body forces, (3) heat conducted into the system, (3) energy radiated into the system (= left-hand side). In this research heat conduction and viscous stresses are ignored. The energy equation can be formulated either by conceptualizing the electromagnetic field *as part of the system* in which case there is no external body force. However one must consider the electromagnetic field energy on the left of the energy balance and the flux of electromagnetic energy $c/(4\pi)\nabla\cdot(\mathbf{E}\times\mathbf{B})$ radiated away (therefore subtracted on the right hand side of the energy balance). Alternatively, one can conceptualize the MHD problem as two subsystems, a mechanical part and a field part, and derive an energy balance on the fluid only (however then one ignores field energy density and flux), but instead one must calculate the work done by the (now external!) ponderomotive force, $c^{-1}\mathbf{v}\cdot\mathbf{J}\times\mathbf{B}$, as well as the Joule heating $=J^2/\sigma$. Strictly speaking one should use the conduction current density $\mathbf{J}'$ seen by the gas to calculate the Joule heating, but for our purposes $\mathbf{J}'\approx\mathbf{J}$. Both terms must be added to the right-hand side of the energy balance.

Thus, there are two entirely distinct ways to conceive of conserving energy for the entire MHD system, but both turn out to give an equivalent energy equation. We prefer to write it using the unified system form, which looks at field energy density and electromagnetic flux. For reference, the full equation (though ignoring line radiation of the gas) would be,

$$\frac{\partial}{\partial t}(\rho e + U^{(em)}) + \nabla\cdot(\rho e\mathbf{v} - p\mathbf{I}\cdot\mathbf{v}) = \nabla\cdot(\boldsymbol{\tau}^{(visc)}\cdot\mathbf{v}) - \frac{c}{4\pi}\nabla\cdot(\mathbf{E}\times\mathbf{B}) + \nabla\cdot(\kappa\nabla T).$$

Here there are no additional forces doing work on the system: e is the specific total mechanical energy of the gas, $e=u(T)+0.5v^2$, $U^{(em)}=(E^2+B^2)/8\pi\approx B^2/8\pi$ is the internal energy density of the field, p is the gas pressure, $\boldsymbol{\tau}^{(visc)}$ is the viscous stress tensor, and κ is the thermal conductivity.

To form a closed system of equations for $(\rho,p,\mathbf{v},\mathbf{B})$ an equation of state of some form is assumed to calculate the temperature form (ρ,p) and the internal energy of the gas is taken to be $u^{int}=u_0+c_v(T-T_0)$, where $u_0=u^{int}(T_0)$ for some reference temperature. For UF$_4$ fuel $M_{UF4}=0.3140225$ kg.mol^{-3}, and $\gamma\approx1.07$, so $c_v\approx R_{UF4}/(\gamma-1)=378.247$ J.kg^{-1}.K^{-1} = 3.78×10^6 erg.g^{-1}.K^{-1}. With appropriate boundary conditions assumed, there are five equations above for eight unknowns. Three equations can be derived from Maxwell's homogeneous equation for $\partial\mathbf{B}/\partial t$. These are the B-field transport equations. Using the generalized Ohm's law approximation, as well as using Maxwell's equation for the current (and ignoring the negligibly small displacement current), so that

$$\mathbf{J} = \frac{c}{4\pi}\nabla\times\mathbf{B},$$

one ends up with,

$$\frac{\partial \mathbf{B}}{\partial t} = \nabla \times (\mathbf{v} \times \mathbf{B}) - \frac{c^2}{4\pi} \nabla \times (\nabla \times \mathbf{B})$$

or because $\nabla \times (\nabla \times \mathbf{a}) = \nabla(\nabla \cdot \mathbf{a}) - \nabla^2 \mathbf{a}$ for any vector $\mathbf{a}$, and noting $\nabla \cdot \mathbf{B} = 0$,

$$\frac{\partial \mathbf{B}}{\partial t} = \nabla \times (\mathbf{v} \times \mathbf{B}) + \frac{c^2}{4\pi} \nabla^2 \mathbf{B} .$$

This completes the MHD equations. For application to shock tube simulations these eight equations can be reduced to a set of five coupled PDEs for (ρ,p,v_x,v_y,B_y).

7.2 *Electromagnetic Shock Tube System*

The 1D-MHD code that has been coupled to MCNP currently employs a current sheet (which could be either formed (1) radially in practice from coaxial electrodes, or (2) as a planar sheet between vertically opposite anode and cathode) and crossed transverse magnetic field at the boundaries of the neutron moderator region to launch MHD waves into the moderator region from both left and right boundaries of the shock tube. These waves build up in intensity until the current and transverse magnetic fields are turned off after some designated time. The details of this gasdynamic/MHD shock production were treated above in the analytic section. The shock production mechanism is however not completely irrelevant to the nuclear modeling. There may be reasons why a particular shock generator will not be suitable. For example, a diaphragm shock tube is too difficult to set up for continuous cycling, and a coaxial quasi-1-dimensional shock tube will not allow efficient fission power production, but a coaxial electrode generator may be used if it can generate a shock strong enough to propagate into a proper gas-filled shock tube region. Many of these issues give rise to questions that can only be answered by at least a 2D magnetogasdynamic simulation, and possibly only by supplementary experimental data. The final project report will eventually comment more upon these questions.

To simulate the shock formation and interaction for a conceptual shock-driven gas core nuclear reactor, the governing single fluid MHD equations were reduced to cylindrically symmetric form with further simplifying assumptions amounting to setting the axial magnetic field B_x=constant. To reduce further to "1½"-dimensional geometry Cartesian coordinates were used to set up the discharge current and associated driving magnetic intensity. Thus, to simulate either a quasi-1-dimensional coaxial shock generator or other Lorentz force type MPD compressor, one needs crossed magnetic field and current sheets, i.e., at the boundary one requires **B** perpendicular to **J** and that *both* are perpendicular to the desired axial flow direction of v_x. Thus, choosing a convention the simulation had $B_z=v_z=0$, and $J_y=0$. The semi-continuous discharge current J_z is then set by using Maxwell's equation and ignoring the negligibly small displacement current, so that

$$\mathbf{J} = \frac{c}{4\pi}\nabla \times \mathbf{B},$$

which is used to set whatever $\mathbf{B}=(0,B_y,0)$ at the tube boundary is required to obtain a given desired current J_z (hence, ponderomotive force).

For the shock tube symmetry then the derivatives $\partial/\partial y, \partial/\partial z \to 0$, $B_z \to 0$ and B_x=constant. Furthermore, in the simulations to be discussed in this report, negligible thermal conductivity and viscosity are assumed, and radiative losses are also not modeled. Under these assumptions the governing MHD equations become,

$$\frac{\partial \rho}{\partial t} + \frac{\partial}{\partial x}(\rho v_x) = 0,$$

$$\frac{\partial}{\partial t}(\rho v_x) + \frac{\partial}{\partial x}\left[\rho v_x^2 + P + \frac{1}{8\pi}(B_y^2 - B_x^2)\right] = 0,$$

$$\frac{\partial}{\partial t}(\rho v_y) + \frac{\partial}{\partial x}\left[\rho v_y v_x - \frac{1}{4\pi}(B_y B_x)\right] = 0,$$

$$\frac{\partial}{\partial t}\left[\rho e + \frac{1}{8\pi}(B_x^2 + B_y^2)\right] + \frac{\partial}{\partial x}\left[\rho v_x(e + P/\rho) + \frac{1}{4\pi}(v_x B_y^2 - v_y B_x B_y)\right] = -\frac{c^2}{(4\pi)^2}\frac{\partial}{\partial x}\left(\frac{B_y}{\sigma}\frac{\partial B_y}{\partial x}\right),$$

$$\frac{\partial B_y}{\partial t} = \frac{\partial}{\partial x}(v_y B_x - v_x B_y) + \frac{c^2}{4\pi\sigma}\frac{\partial^2 B_y}{\partial x^2}.$$

This form is fairly easily to put into discretized form. However, by converting to a rationalized Gaussian system of units the constants c and 4π can be eliminated from the equations thereby allowing an even more convenient discretization for computer coding. Specifically, looking at the energy equation it is clear that defining,

$$\mathbf{b} = \frac{\mathbf{B}}{4\pi},$$

we can eliminate 4π. Then, by setting,

$$\varsigma = \frac{4\pi}{c^2}\sigma,$$

we can entirely eliminate the constant 4π from all the equations. Note that this amounts to also redefining the electric field as Ξ, and current density as χ, which can be computed directly from $\mathbf{b}$ and ς using the Gaussian formulae with $4\pi \to 1$, and $c \to 1$, and can be related to the conventional Gaussian system $\mathbf{E}$ and $\mathbf{J}$ by the following relations,

$$\Xi = \frac{c}{\sqrt{4\pi}}\,\mathbf{E},$$

$$\chi = \frac{c}{\sqrt{4\pi}}\,\mathbf{J},$$

For example, the ponderomotive force law, $\mathsf{F}^{em} = c^{-1}\mathbf{J}\times\mathbf{B}$, (for a neutral plasma) then becomes just, $\mathsf{F}^{em} = \chi\times\mathbf{b}$, in the new rationalized units. Note that in converting to these units the only drastic change is that the electrical conductivity s has different dimensions, in Gaussian units $[\sigma]=\mathrm{s}^{-1}$, whereas in the new system $[\varsigma]=\mathrm{cm}^{-2}.\mathrm{s}$, or equivalently one can consider the resistivity $\eta=1/\sigma$, which has dimensions of Time in the cgs system, now has dimensions of $[\mathrm{Length}^{2}.\mathrm{Time}^{-1}]$ or units of $\mathrm{cm}^{2}.\mathrm{s}^{-1}$ in the new system where c^2 and 4π do not appear. As a quick example, consider the scalar electrical conductivity of a steady state UF_4 plasma at P=1 atm, T=2000$^{\mathrm{o}}$K roughly, then $\sigma\approx1.0$ [Siemens$\cdot$m^{-1}] from data in MKS units, which is $\sigma\approx8.98\times10^{9}$ [s^{-1}] in Gaussian (cgs) units. But in the new rationalized system used for computer coding we would use $\varsigma = 8.98\times10^{9}.4\pi/c^2 = 1.69\times10^{-5}$ [cm^{-2}.s] in the new units. In other words the electrical resistivity that needs to be used for the computer code would need to be set about $c^2/4\pi \approx5.3\times10^{14}$ times *larger* than the conventional electrical resistivity of the plasma in Gaussian units. With these modifications taken into account, the system of equations for computer discretization in conservative form are further simplified.

The key thing to note is that the non-electrodynamic variables ($x,t,\rho,\mathbf{v},e,P$) are still in Gaussian units of g, cm, s. The new variables *only* affect the appearance and dimensions of the *electrodynamic terms*. As a final note before describing the computer code used to solve these equations, it should be remarked that strong shocks are capable of ionizing gases, and across electrical discharges in gases the conductivity approaches that of a fully ionized plasma: therefore, it is not too extreme, for the application that this report is concerned with, to make the approximation of infinite electrical conductivity, then $1/\varsigma \to 0$: hence, the diffusive terms in the last two equations may be ignored as a rough approximation. Of course simulations hoping to capture energy efficiencies for the processes involved obviously cannot make such a rash approximation; indeed, such goals are not really compatible with neglect of thermal conductivity, viscosity and radiative losses. Such features of realistic shock tube processes are, however, deferred to possible later stages of research for the current project.

7.3 *Solution of the MHD Shock Tube Equations*

Although the report does not cover the numerical method used to solve the above equations. However some brief comments will be given where appropriate to note the particularities of the numerical algorithm written in Fortran code that was used to obtain the results reported on in Section 8. One complication in particular frustrated efforts to use a full flux-corrected transport MHD solver algorithm. The MCNP code consumes considerable CPU time each time it is called, therefore to limit simulation run times to days rather than weeks the MHD code was allowed to run for a given number of time steps and/or simulation physics seconds before pausing to call MCNP for updating the fission power and neutron flux source terms. In addition, for adequate convergence in the MCNP tallies, the shock density profile had to be collapsed into just a few cells, where the shock waves gave steep density profiles the MCNP file input writer script made the collapsed cells finer, but where the density varied slowly many cells of the fine MHD grid mesh would be merged into one or two large cells. This made the fission power density q''', and neutron flux Φ_n, calculations rather crude. It was decided therefore that the fission source term in the energy equation would not be added to the MHD solver algorithm until the coupled codes could be verified as accurately reproducing the MHD-shock simulation profiles for a non-fissioning gas. The intent was to proceed to include the fission power source term (as well as the fission-fragment and neutron flux ionization enhancements to the electrical conductivity) but all efforts to debug and validate the modified MHD code and script programs failed to culminate in time to allow a further round of debugging and testing of the fully coupled MHD-MCNP code with fission source term feedback.

A leapfrog trapezoidal algorithm (LFT) was used for transporting the fluid variables a given time step. The main difference between gasdynamic LFT and the MHD LFT used in this report is that the MHD system includes additional wave speeds, the fast and slow magnetoacoustic waves, as well as Alfvén waves. Details of leapfrog trapezoidal algorithms for MHD and flux-corrected transport methods can be found in the references [9, 10, 11, 12, 13]. There is also a time scale characteristic of magnetic field diffusion that affects the stability of the solution. The fast wave velocities along with the gas dynamic acoustic wave velocity were used to determine the allowable maximum time step dt_1 for a fixed spatial mesh size dx, consistent with CFL stability. The time scale for magnetic field diffusion was then set as $dt_2 = 0.5 dx^2/\varsigma$, where ς is the electrical resistivity defined above. The time step for each iteration of the MHD equation solver was then taken as $dt = \min(dt_2, dt_1)$.

The remainder of this section considers the task of coupling the MHD code to the general purpose Monte Carlo neutron transport code MCNP4C that was used to calculate fission power source terms and neutron flux in the shock tube and surrounding BeO moderator material.

9[9] D.L. Book, J.P. Boris, and K. Hain,, "Flux-Corrected Transport. I. SHASTA, A Fluid transport Algorithm that Works", *J. Comp. Phys.*, **11**, 38-69, 1973.

[10] D.L. Book, J.P. Boris, and K. Hain,, "Flux-Corrected Transport. II. Generalizations of the Method", *J. Comp. Phys.*, **18**, 248-283, 1975.

[11] J.P. Boris, D.L. Book,, "Flux-Corrected Transport. III. Minimal-Error FCT Algorithms", *J. Comp. Phys.,* **20**, 397-431, 1976.

[12] S.T. Zalesak, "Fully Multidimensional Flux-Corrected Transport Algorithms for Fluids", *J. Comp. Phys.,* **31**, 335-362, 1979.

[13] C.R. DeVore, "Flux-Corrected Transport Techniques for Multidimensional Compressible Magnetohydrodynamics", J. Comp. Phys., **92**, 142-160, 1991.

7.4 *Modifications to the MHD Code for Serialization with MCNP*

The general purpose Monte Carlo code MCNP4C is suited for high precision physical modeling of fundamental radiation interaction phenomena. It is less suited for dynamic system simulation, where a discrete ordinance code might be favored. Nevertheless, in the nuclear engineering community MCNP is a favored tool; hence, it was chosen for use in this project. The main difficulty in using MCNP for the shock-driven reactor system modeling is that it takes many minutes for MCNP tallies (Monte Carlo schemes all involve tracking individual particles and building up statistics from such primitive numerical trials) to converge to within reasonable tolerances. But the MHD simulation code updates the gas pressure, temperature and density roughly every microsecond. Yet the shock waves travel at finite velocity, hence for accurate fission power calculations the MCNP code needs to be called many times during a reactor simulation cycle. With some 2000 to 10,000 time steps typical for the Leapfrog trapezoidal MHD solver it immediately dawns upon the simulationist that it will be untenable to update the fission power source terms every step of the MHD shock evolution. Therefore, some criterion, or set of criteria, is needed to determine judiciously when to pause the MHD code to call MCNP to update the fission power terms. For this report a combination of a minimum lower gas density (below which fission events could be regarded as negligible) and a minimum time in seconds over which the density profile would not change too rapidly and yet exceeding an average neutron lifetime in the gas were the chosen criteria. However, even these conditions often resulted in excessively slow simulations, so a third criterion was used, which was to explicitly limit the maximum number of times that MCNP is called to a fixed number over the entire simulation cycle.
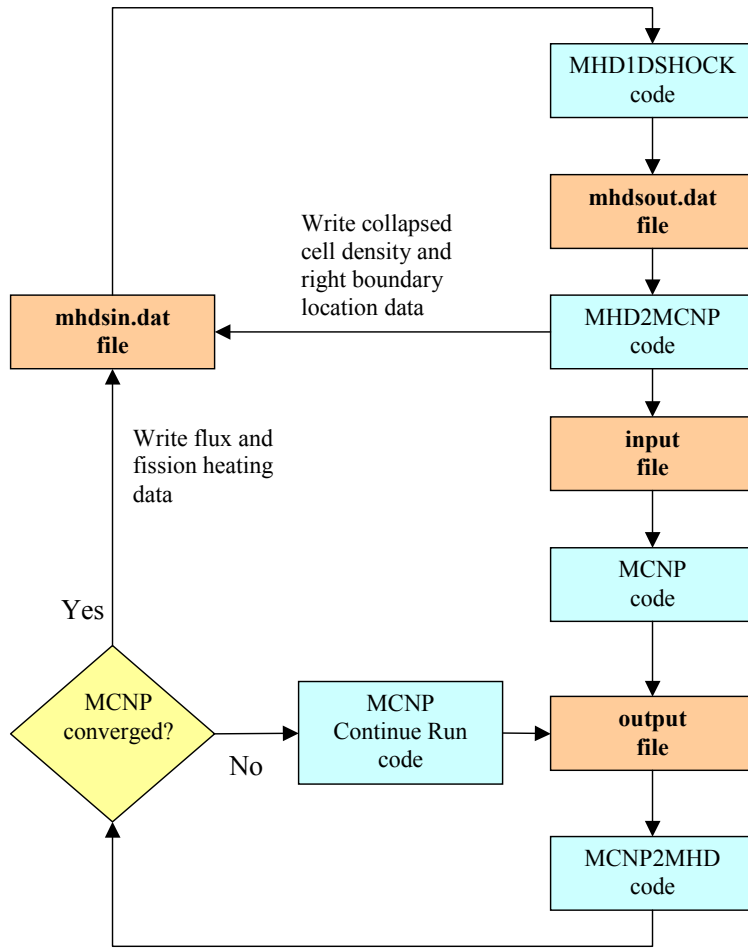
Figure 4. Flow diagram of operating script to control simulation linking MHD1DSHOCK and MCNP.

This logical loop is maintained until the MHD1DSHOCK code completes the interaction of the two shock waves or reaches its maximum assigned integer time step (or computer memory is saturated).

Serialization of the MHD and MCNP codes, therefore, involved writing a Linux script program to coordinate the following executable tasks: (1) starting the MHD code and (2) running it until the conditions required for calling MNCP are attained, then (3) preparing input cards for MCNP on-the-fly using intermediate program codes, then (4) running MCNP, (5) checking for convergence, if it hasn't converged then (6.1) keep running MCNP, then (6.2) upon convergence preparing an input card for the MHD code to (7) resume from the previous time step, and repeating steps (2)-(7) until the MHD code finished a cycle (reached it's maximum set time step.) A flow diagram of the script logic is shown in Figure 4.

7.5   *Getting the Coupled Codes Started*

The most acute sensitivities of the simulation results to input parameters are the electrical conductivity and neutron source strength. Low conductivity, or high resistivity poses a problem because it sets the time scale for magnetic field diffusion. If the magnetic field is large at the boundary grid cells then sudden changes in intensity can lead to anomalous numerical results such as negative pressures being produced. The neutron source strength is adjustable and easy to deal with, so if either the fission power density or neutron flux exceeds the compiler single precision maximum for floating point numbers then (implying an unwanted highly supercritical core) one can lower the ambient source strength. These peculiar problems will be dealt with in Section 7.6. For now we will discuss the practical details of finding good starting conditions.

As of the present date the codes function together well, but the user must exercise care in selecting the input parameters described above in Appendix Table 7. One must ensure that the MCNP pre-processor does not collapse the data from the MHD fine grid mesh into a single cell, because this can cause problems for the MCNP post-processor or MHD pre-processor. This can happen if MCNP is called early on in a simulation before the gas density starts to get perturbed by the shock generator. This problem gets amplified when the MHD simulation time step is very small and of the order of 10's of nanoseconds. With such very small time steps the shock generator has not had time to produce significant shock wave build-up of gas density, so the pre-processor is in danger of collapsing the grid to a single cell. This will be amended in future versions of the scripts. However it is nevertheless interesting to examine how such small time steps can arise, because they are symptomatic of another problem: resistive shock instabilities. That is, the resistive shocks at high Mach numbers encounter physical instabilities. In the actual physical problem, as a wave steepens and its scale becomes smaller than the resistive scale length, other dissipations with shorter scale lengths will be needed to prevent the nonlinear growth of the wave. So either viscosity or other transport will be needed or in doing numerical simulations numerical diffusion can be increased by increasing the grid size or other means.

Section 7.6 will discuss some of these peculiar problems. General comments on how to get the codes started and running together will now be summarized.

7.5.1   Finding Sensible Initial Conditions and Inputs

Physical sensibility and research interests should determine ambient pressure and density "Pin", and "rhoin" in Appendix Table 7. Magnetic fields cannot exceed megagauss intensity (and even then only for short pulsed fields) so there are physical limits that determine reasonable shock-drive boundary conditions "byi" in Appendix Table 7. The neutron source strength cannot reasonably be much in excess of 10^{20} neutrons per sec, because even accelerator driven systems would be pushing practical limits to provide such and enormous quantities of neutrons. It takes anywhere between 5 to 20 minutes to run one call to MCNP, so is unreasonable to set "ncallmcnp" to much more than 100 to 200 calls for rapid benchmark research. Given (as discussed later) the number of time steps required to see the two shocks collide can be in the 10's of thousands, one clearly should limit the total number of times MCNP will be called by basing calls to MCNP upon either real (simulation) time in seconds, or upon ncallmcnp. One can always run the coupled code script and use the system's keyboard kill command to quit a simulation early if it looks like the shock collision has been captured.

Once a desired et of input parameters has been selected the best way to run a simulation is to first turn MCNP off by setting "ismcnp=F" in the namelist file 'mhdini.dat'. One can set a very large maximum time step, say "nend=100000" in this case, and wait a few minutes to see the results. Note that with MCNP thus turned off it is simpler to run the MHD code without going through the Linux shell script, just run the native MHD executable.

If negative pressures which are a symptom of resistive shock instabilities, are encountered then, generally, if one wants to keep the same shock tube length, resistivity and grid resolution, then one needs to either, (i) artificially reduce the maximum allowable time step by reducing the fraction "diff_tscale", or, (ii) decrease the applied magnetic field by decreasing "byi", to reduce the magnetic Reynolds number. It's a matter of trial and error. However, by choosing option (i) to decrease diff_tscale, one may in effect reduce the time step *dt* set by the subroutine SETDT to such a small value (maybe even nanoseconds) that the simulation stops before the shocks collide. To avoid missing the shock collision one has to inspect the simulation (again with MCNP turned off) to see if with the smaller time steps the simulation does indeed advance far enough to produce a collision, if not then one must increase "nend" to get more total time steps.

If no negative pressures are seen (and of course of sufficiently strong shocks were produced) then the inputs are probably fine and one can set "nend" to roughly twice the time step at which one saw the shocks collide (to get a decent history of the post collision evolution). Then turn MCNP on by setting "ismcnp=T" and run the shell script again and wait for the full results of the coupled MHD-MCNP codes.

For smoother (less discrete) fission power and neutron flux data one can increase the number of times MCNP is called by either increasing "ncallmcnp" or decreasing "dtmcnp".

7.6 *Trouble shooting the Simulation Codes*

The peculiar problems encountered while testing the MHD1DSHOCK and MCNP4C coupling are now described.

7.6.1 MCNP4C Convergence Criteria

To force MCNP to converge rapidly one can do two things,

   (1.1) One could collapse a lot of cells from the MHD mesh to just a few, averaging out the gas density. This will mean MCNP will not have to wait too long for sufficient tallies to build up in each cell. To do this edit the file 'mcnpprob' and change the ninth number in the line,

```
mcnpspec 1 1 20 0  0.005 0.05 0.05  40 1.0 62.5
```

the fifth number here is the maximum permissible standard deviation for k_{eff} that MCNP uses to determine convergence. Ideally for high statistical confidence, the maximum standard deviation should really be around 0.005 or less, however smaller values will drastically slow down the simulation (by requiring more cycles be simulated in MCNP for better statistics). The sixth and seventh numbers are the maximum permissible standard deviation in the flux and fission heating tallies respectively for individual cells.

(1.2) One can also specify a statistically large maximum permissible standard deviation for k_{eff}. This is done by editing the file 'mcnpprob'. At the line,

```
mcnpspec 1 1 20 0  0.005 0.05 0.05  40 1.0 62.5
```

the fifth number here is the minimum standard deviation for k_{eff} that MCNP uses to determine convergence. Ideally for high statistical confidence the min. standard deviation should really be around 0.005. For scoping calculations, perhaps a larger value is better, at least until debugging of other aspects of the code can be accomplished.

7.6.2 Problems with High Resistivity Plasmas

Two of the most serious problems occur for simulations of high resistivity plasmas ("res"~10 or higher). For instance, in a highly resistive plasma, when there is virtually no shock, only a very weak linear wave motion at the beginning of a simulation, then the MHD transport algorithm time step is dominated by the magnetic diffusion time $dt_{diff} \sim \varsigma dx^2$, where $\varsigma = 1/res$, is the gas conductivity [cm^{-2}.s] in rationalized Gaussian units. So for high resistivity the diffusion time is small, and if diffusion dominates fluid advection (as will be the case early on before high speed shocks are formed) then this time step can be significantly smaller than the time step governing advection that satisfies the CFL condition. Hence a simulation can advance a large number of time steps yet only a very few seconds, maybe only a fraction of a microsecond. (This will often lead to the problem of total cell collapse during coarse grid generation mentioned above.)

A more serious problem can occur when the mesh size is large—perhaps because one is trying to increase the allowable time step governed by time $dt_{diff} \sim \varsigma dx^2$. Notice that when the magnetic Reynolds number is large (strong *B*-field diffusion/weak advection) then dt_{diff} must be used to set the simulation time scale for numerical stability. If one does not use dt_{diff} then negative pressures will result from diffusion of the strong magnetic field at the boundary of the grid that simulates the shock generator. This may be avoided in future updates of the MHD1DSHOCK code by smearing out the pulse current shock source over more grid cells. But one can still encounter negative pressures when the shock generating magnetic field is turned off. The magnetic field should evolve self-consistently when the boundary conditions imposed change from the strong applied shock-driving field to continuous boundary conditions. But if the grid spacing is too small then when the boundary conditions are changed in this manner, at a single time step, it can cause the magnetic field to diffuse too fast for the simulation time step (which is now being governed by the advection from the fast shock waves that have been produced). One needs either a non-global time step that differs for different regions in the gas depending upon the local dominant transport process, or one must protect against negative pressures resulting by increasing the coarseness of the grid, making *dx* larger but for the same shock tube length, by reducing the number of grid points, alternatively one could place a multiplicative scale factor in $dt_{diff} \sim \varsigma dx^2$, such as $dt_{diff} \sim 0.1 \varsigma dx^2$, in order to reduce the simulation time step artificially. This factor is tunable and is set through "diff_tscale" in the namelist file 'mhdini.dat', so the diffusion time step is defined as dt2=diff_tscale*dx*dx/res, in the subroutine SETDT. The actual time tep used in the solver routine STEPON is the minimum of this dt2 and "dt1" obtained from the CFL condition on the wave velocities. Either fix might avoid negative pressures, but this is not a universal panacea for this problem.

In practice the negative pressures damp out and disappear after a few time steps once the transverse applied field at the boundaries is allowed to relax. A problem is that there is a serious effect on the fluid variables: One can get gas densities nearly an order of magnitude greater for the exact same initial conditions and settings whenever the diffusion problem is encountered and the pressures go negative near the boundaries. So the integrity and validity of the entire simulation becomes suspect. By changing the length or time scales to avoid negative densities one gets (for the exact same inputs otherwise) a much lower peak density (and lower peak pressures and temperatures as well). For most of the case studies presented in Section 8 of this report, inputs and initial/boundary value conditions were chosen to avoid negative pressures. This can be done without too much expense by running the MHD1DSHOCK code with calls to MCNP turned off. This runs the code very quickly (run times typically in minutes on a Pentium desktop) and one can inspect for negative pressures. If the pressures are positive globally then the code can be rerun with MCNP turned on, which takes many hours to run.

A more permanent fix for these shock tube simulation issues will be attempted in future code versions. One solution for example might be to use a smoother shock generation transverse magnetic field, one that does not get switched from applied field at the fluid boundary to continuous boundary condition at a single time step, but rather a shock driver that relaxes over a few time steps. This would be a more pleasingly physical resolution after all. However, it does not mean that the essential difficulty with the numerical algorithm should be ignored. One would like to avoid negative pressures irrespective of how the boundary conditions are applied, as a matter of principle and simulation programming hygiene!

Although not comprehensive, here just a few of pertinent issues that arose, during code debugging and simulation testing. The first two deal with getting the simulation to run more efficiently and avoiding nonphysical results like negative pressures. The last topic here deals with engineering matters on how to simulate greater fission energy release.

In summary, if you set the input variable "res" to a large value (cm^2/s) in the file 'mhdini.dat' then you might expect magnetic field diffusion to dominate over fluid advection initially in a simulation before strong shocks start to form. This gives a different characteristic time $dt_2 \sim 0.5 dx^2/\varsigma$, that governs numerical stability in the presence of diffusion in magnetic field transport. If negative pressures result when ς is large therefore one should do either or one of at least four things:

(1) Increase the shock tube length sx, to increase dx, keeping the number of grid cells fixed (making a coarser mesh).

(2) Decrease the number of grid points mx, (again to increase dx by making the mesh coarser).

(Either of these will give larger diffusion times, making it more compatible with the default dt_1 from the CFL condition. However these are not guaranteed to fix the negative pressures; for a fine resolution, one needs some other fix.)

(3) If you want a fine mesh then you can artificially decrease the diffusion characteristic time, say by setting $dt_2 = 0.1*dx*dx$/res, in the source code 'subroutine setdt', or similarly adapting the scale for diffusion. Because the simulation time step for the leapfrog algorithm is set to dt=min (dt_2, $dt1$), where dt_1 is the CFL time step from the wave velocities, this should ensures a time step that avoids unphysical pressure perturbations from strong diffusion. To avoid negative pressure entirely for high resistivity trials one really should add extra code to adapt the time step whenever negative pressures are seen, so that the code recalculates the transported fluid variables with a smaller time step. (This should be done be rewinding the simulation, so that the previous time step variables are not over-written before this inspection of the pressures is made). Note that flux-correction should be able to avoid negative densities, so generally you should only be worried about the pressure as far as problematic diffusion scales become evident.

(4) Finally, one can reduce the magnetic Reynold's number by decreasing the intensity of the applied tranverse magnetic field by decreasing the input "byi". However, if the applied shock-drive field is too low then now shocks will form and the purpose of the simulation is defeated! So one must in practice run the MHD1DSHOCK code with MCNP turned off to perform rapid testing of initial conditions to see what sort of magnetic field and pulse time is required for adequate looking shock build-up intensities, making sure that the simulation runs long enough to capture the shock collision. Then as long as no unphysical negative pressures are encountered one can run the script for the coupled codes with MCNP turned on.

7.6.3   Low Fission Power Output

To boost the fission power production one can either increase the ambient neutron population available for multiplication in the pulse (most likely by adding an extraneous neutron source, set by the input "source", which is interpreted by MCNP as ambient neutrons per second), or increase the size (physical dimensions of shock tube radius) of the reactor, or increase the uranium enrichment or add plutonium (or even add very small quantities of americium) to the fuel, which have the effect of increasing k_{eff} and also the neutron multiplication factor in the pulse.

   (1) To increase uranium enrichment, edit the file 'mcnpfix', go to the line,

```
m1 92235.61c 0.1 92238.61c 0.9 9019.60c 4.0 $default core material
```

and change the fraction after 92235.61c to 0.95 say for 95% enriched fuel, then you must change the fraction after 92238.61c accordingly to 0.05.

   (2) Increasing the reactor size. To increase the shock tube radius, edit the file 'mcnpfix', at the lines,

```
begin surfaces
    1 cx    50
    2 px -50
    3 px   50
   10 cx   100
   11 px -140
   12 px   140
end surfaces
```

that go into writing the MCNP surface card, "1 cx 50" means a radius of 50cm. So to model a 160 cm diameter reactor change "1 cx 50" to "1 cx 80". But then you must also give the reflector wrapped around the shock tube more room, so add the difference to the number at surface 10, so change "10 cx 100" to "10 cx 130" for the 160cm diameter change.

(3) Increasing the neutron source. We found that the shock-driven simulation requires a large background neutron population for multiplication in the pulse in order to obtain a useful amount of fission power. In a real shocktube reactor, the neutron population available for multiplication in the pulse will be a result of delayed neutrons from decay of a population of delayed neutron precursors generated and sustained by earlier pulses. Extraneous neutron sources may also be added to increase this population available for multiplication in the pulse. So, to model a background neutron source the parameter "source" is specified in the 'mhdini.dat' file. For example, set,

```
source=1.0E+10
```

in the namelist file 'mhdini.dat' to model a background neutron source giving isotropic neutron source strength of 10^{10} neutrons/sec. If the peak gas density is about 0.1 g/cm^3 then a strong neutron source is recommended to boost fission power production, say: source=1.0E+15.

The simulation records, as a function of time, the system (effective) neutron multiplication factor, k_{eff}. MCNP4C determines k_{eff} by Monte Carlo numerical trials, so it is determined statistically from tracking many neutrons through the system. Now, the point of this is that it is possible for k_{eff} to increase well above unity when the fissile fuel density becomes very large and a lot of mass is compressed into the reactor core region. This can at sufficiently high levels lead to "run-away reactor" and a supercritical chain reaction, which is the purpose of the shocktube reactor design since fission power is generated in short bursts through the multiplication of existing neutron sources in the pulse. There is no danger involved in this scenario since first, it is difficult to achieve the gas densities necessary for the super-critical state but also because there is a limit on the total amount of fissile gas available in the system. However, more importantly are all the negative reactivity feedback effects that will lower k_{eff} eventually bringing it to a subcritical state before the next pulse. These effects are largely derived from the increase in temperature of the gas leading to Doppler broadening affecting resonance escape probability but more importantly decreasing the density of the gas in the pulse. One potential simulation problem can result if the ambient neutron source strength in the shocktube available for multiplication in the pulse is set too high. In this case, the multiplication in the pulse can cause the neutron population to grow to very large numbers leading to floating-point number overflows in the neutron population scale factor "noft" which will crash the simulation. In which case, the same input parameters might be selected again, but with lower neuron source strength.

7.7   *Shocktube Modeling in MCNP*

7.7.1   Purpose of the Model

At each step during the propagation of the shockwaves and throughout their interaction, the fissile gas and neutron population are contributing to alter the intensive properties of the medium through nuclear interactions. At a minimum, it can be understood that these interactions affect temperature and molar concentration of various species including fissile material, fission products, ionized species, etc.—namely through the fissioning of the fissile gas and the ionizations resulting from neutron and fission product interactions with the medium.   Magneto-gas dynamic modeling of the shockwave propagation and interaction is a challenging problem in itself. The additional complexities associated with modeling the simultaneous nuclear interactions only make the problem more difficult. Therefore, it was decided to develop a series of computer codes to integrate the magneto-gas dynamic computer code, MHD1DSHOCK, to model the shockwave propagation and interaction and the general Monte Carlo nuclear transport code MCNP5 to model the nuclear interactions. These codes are run in series over a specified time step (and later by a more physical criterion[14]) to update the magneto-gas dynamic and nuclear parameters before progressing to the next time step (see Figure 1).   There is no reason why the nuclear code cannot be run after each single time step of the MHD code, but for practical reasons this would result in a very long simulation run time, and is probably unnecessary because the time scale of the MHD code time step is likely to be much smaller (set by the CFL condition) than the typical neutron lifetime. The supporting theory and modeling implemented in each code is described below as well as the pre-/post-processor codes that facilitate the communications between MHD1DSHOCK and MCNP at each time step.

---

[14] The MHD code can halt to call MCNP after a fixed time step, but other more physical criteria have been implemented as well, so that MCNP will update the fission power and neutron flux based upon one or more criteria. Three proposed criteria (which could be used simultaneously) are (1) when the maximum velocity in the gas would transport a particle by more than a neutron mean free path (this is currently *not* implemented), (2) when the gas density in any cell changes by a significant percentage sufficient to warrant updating the nuclear variables (this has been implemented), (3) whenever the elapsed time since the previous call to MCNP approaches a few times the neutron lifetime (this has been implemented too). If any of these criteria are true then the MHD code will halt to let MCNP run.

7.7.2 Shock Tube Model-Nuclear Code

The shocktube is modeled as a cylinder parallel to x, y, or z-axis with its center point fixed at the coordinates (0,0,0). Any differing coordinate system utilized by the MHD1DSHOCK code is accommodated by the intermediate code MHD2MCNP that prepares the MCNP input based on the MHD1DSHOCK output (for example the MHD coordinate system origin is indeed at the left boundary rather than the shock tube center). A number of fixed MCNP input cards are supplied in the input file, MCNPFIX, which provide the general setup of the problem and are located here for convenience since small routine changes and additions can be made without modifying the MHD2MCNP processor code. Further, the MCNPFIX file contains all the information on the geometry and materials external to the shocktube including the end regions and the radial reflector and materials including coils, magnets, and any other structural components.

The interior of the shocktube is subdivided into cells axially according to the cell structure supplied by the MHD1DSHOCK code. Attempts are made by MHD2MCNP to collapse the fine cell structure of the MHD1DSHOCK code into a smaller set of cells for use in the MCNP calculation (see Figure 5). The criterion for collapsing cells is based on the relative change in density from one cell to the next. Specifically, if the maximum relative difference between two cells is less than some user specified value, then the two cells are marked for collapse according to the following criterion,

$$\frac{\left|Rho_i - Rho_{i+j}\right|}{\min(Rho_i - Rho_{i+j})} \leq dblMaxRhoDiff$$

where i is the left-most cell for collapse and j is a successive cell for comparison.

Comparison is then made with the next adjacent cell comparing to the original, left most cell in this series of collapsing until the maximum relative difference between the current cell and the left most cell exceeds *dblMaxRhoDiff*. Then a new series of comparisons are begun starting with the cell with relative density that exceeded *dblMaxRhoDiff* in comparison with the original left-most cell in the series collapsed. So for example if *dblMaxRhoDiff* is 1.0, cell collapse will continue until the density of a successive cell differs from the starting cell by double or half and excluding that final cell where the density was greater.
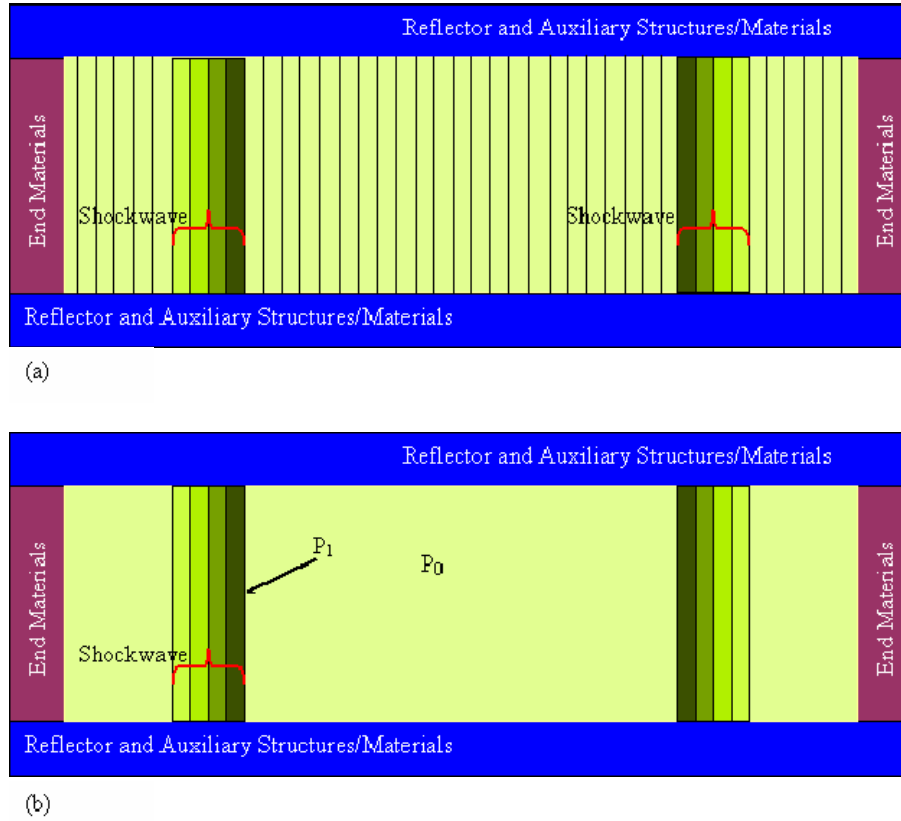
Figure 5. Shocktube models used in the combined simulation codes.

a) Illustration of the shocktube model output by the MHD1DSHOCK code with many cells. b) Illustration of the shocktube model after cell collapse by MHD2MCNP where many of the cells with nearly the same density/pressure are collapsed to simplify the MCNP model

By decreasing the parameter *dblMaxRhoDiff* one then gets finer and finer coarse meshes until eventually the entire MHD grid resolution is resolved, increasing *dblMaxRhoDiff* produces coarser meshes until eventually the routine collapses the entire domain to a single cell with density equal to the average over the MHD grid. In this manner an adaptive mesh/cell spacing scheme is enabled to capture the fine details of the shockwave profile and also reduce the computational burden of tracking many cells in MCNP.

In collapsing successive cells, the macro cell created has the volumetric average density of the micro cells of which it is comprised. The new cell densities along with their cell number and location of the right bounding surface are written to a file MHDSIN.DAT for later use by the post-processor code MCNP2MHD and the MHD1DSHOCK computer code itself for the next time-step. Also, the cell volume and the area of the left and right bounding surfaces are calculated and written on VOL and AREA cards added to the MCNP input file specification and are required in calculating flux and fission heating tallies for the cells and surfaces comprising the shocktube core.

7.7.3 Calculation of k_{eff}, Neutron Flux and Cell Heating

The neutron multiplication factor, k_{eff}, as well as a number of tallies are made by MCNP to predict the neutron flux (per cm^2-sec) and heating due to fission energy release (MeV/g or MeV/cm^3) in each cell. MCNP executes the problem defined by the MHD2MCNP pre-processor code and runs for a specified number of histories. The post-processor code MCNP2MHD examines the output and determines if the problem has converged, that is to say it has achieved the user specified accuracy for k_{eff} and the several tallies for flux and fission heating. If the maximum allowable standard deviation is exceeded for k_{eff} or any of the cell tallies, then the problem is continued for an additional user specified increment set from the problem specification file, MCNPPROB, and continues in this fashion until k_{eff} and all tallies meet the required accuracy.

Flux is estimated by a track-length tally (type F4) for each cell defined in the MCNP input file. Because the adaptive mesh/cell spacing scheme can produce very thin cells in trying to capture the potentially sharp shockwave profile, a surface estimate of the flux (type F2) is also tallied at the left and right boundaries of each cell. For very thin cells this should provide a better estimate of the flux and reduce the number of *Continue MCNP* runs that must be executed in order to obtain the specified user accuracy.

Cell heating due to fissioning is estimated using a type F7 tally which measures the energy deposited from fission in units of MeV/g for a cell. Alternately, volumetric heating in units MeV/cm^3 can be selected as an option on the problem specification file, MCNPPROB. Gamma rays from fission are included in this tally by counting them as being deposited locally at the site of fission. Additionally, a modified surface flux tally (type F2) is used to obtain fission heating estimates for very thin cells as discussed above for flux estimation. Here a tally multiplier is specified to account for the correct material densities, fission cross-section MCNP reaction number, and energy from fission MCNP reaction number.

7.7.4 Post-processing of MCNP Output and Preparation for Next Time-Step

The MCNP2MHD post-processor code examines the MCNP output after the initial and each subsequent Continue MCNP run (if any) to check the accuracy of the estimates for k_{eff}, flux tallies, and fission heating tallies. If the estimated error is within the user-specified limits for each, then flux and fission heating tallies are extracted from the MCNP output file and appended to the MHDSIN.DAT file initiated by the MHD2MCNP pre-processor code. Additionally, the neutron population for this time-step is updated based on the new k_{eff} and prompt neutron lifetime (l_n) calculated by MCNP for this time-step and according to the following formula,

$$N(t_n) = N(t_{n-1})e^{(k_n-1)\Delta t / l_n} + \frac{S \cdot l_n}{k_n - 1}(e^{(k_n-1)\Delta t / l_n} - 1)$$

where, n is the nth time-step, Δt, and $t_n = t_{n-1} + \Delta t$; S is the background neutron source strength in neutrons/sec.

This neutron population is used by the MHD1DSHOCK code to scale the flux and fission heating tallies since each of these are normalized to 1 starting neutron. Because of cell collapsing in MHD2MCNP, the cell structure of the MHDSIN.DAT file will differ from that originally output by the MHD1DSHOCK code in MHDSOUT.DAT and used in the subsequent time-step, interpolation on the coarser MCNP grid is required. As a result of the interpolation scheme used by the MHD1DSHOCK code, a minimum of six interpolation points/cells are required in MHDSIN.DAT.

One reason for coupling the MHD-gasdynamic simulation code with the MCNP neutron transport and fission power tally code is precisely because the neutron flux depends upon the multiplication of the neutron population $N(t)$ in the previous time step, so one needs the full simulation history to determine how the fission power will vary. That is why one cannot simply run the MHD shock code and capture frozen instants from the simulation and run an MCNP calculation for that instant to determine fission power output, one would not know what absolute neutron number density to use as the input in such a scenario. These isolated criticality simulations give neutron flux and fission heating relative to one source neutron. So there is really no escaping running the codes as a coupled simulation. The only alternative would be to build up a massive database of neutron flux and fission power as functions of many gas density profiles and histories. This is almost certainly a task that would take as long as or longer than simply running the two codes together in series with each updating input data for the other as time is advanced.

Preliminary Investigations

A preliminary investigation was made into the methods available to characterize the reactor core. To begin with, a simple model of a reactor core with one homogenous region was setup in MCNP. This was modeled as a 3 m^3 right-circular cylinder with an additional 40 cm BeO reflector (see Figure 6 and Figure 7). The fissile gas was assumed to be UF$_4$ at 5 MPa partial pressure and 4000 K. The temperature was selected partly based on parsimony, since it requires excessive work to incorporate temperature dependent cross sections into MCNP.[15] It was first sought to characterize the neutron spectrum in various regions of the reactor. The core was subdivided into three regions from the inner to the outer core region and the reflector into two regions, inner and outer. To get a detailed spectrum, 482 energy groups was setup by thinning the energy grid from the ^{235}U library used in the calculation. New high temperature libraries processed from NJOY99 were used for this evaluation. The MCNP kcode was setup to run 100,000 histories in each of 200 cycles for a total to 20 million histories. Track length estimations of neutron flux were made using tallies for each subdivided region. The preliminary calculations showed that the spectrum becomes slightly harder moving toward the core center as expected. Detailed examination of smaller ranges of neutron energy showed a rather poor characterization of the flux particularly near resonances. For this reason the energy grid will be reevaluated to redistribute or add points in these regions for future models.

---

[15] For a full simulation the MHD code will keep track of the true gas temperature that effects density and pressure. If required at a later stage of research then variable temperature effects (Doppler broadening of resonant for fission and capture) can then be incorporated, though it should be noted that this is not a trivial task and requires significant computer memory to be permanently allocated for the cross section libraries.

Some interesting but unexpected results were obtained when modeling the criticality of the shock tube as described in the earlier sections above. A negative reactivity feedback effect was noted for two approaching shockwaves. This was modeled for the simulated case of two shockwaves of unvarying characteristics as they approach each other from opposite ends of the shock tube. That is to say that the strength and profile did not change until they interact at the center of the shock tube. It was only then when they interact and collide that a positive reactivity is noted and the shock tube core went prompt critical. The reason for the negative reactivity associated with approaching waves relates to the effect of the reflector region and is analogous to the self-shielding effect noted for the lumping of fuel to form a fuel/moderator lattice and can be explained as follows. The rather thin/flat disk geometry of the shockwaves is such that the leakage from a shock wave is large in any configuration. When the shock waves are far apart, there is a high probability that neutrons escaping a shock wave will enter the reflector and slow down in energy before being absorbed in one or another shock wave there by increasing the resonance escape probability. However, as they approach each other, the probability increases that neutrons leaking from one wave will be absorbed in the other wave before slowing down. It is only when the waves collide and experience a non-linear increase in density/pressure do we see an increase in k_{eff} since the more compacted, collided waves have a smaller total leakage term than the two waves separately. This negative reactivity behavior of approaching shock waves might be altered by adding a moderating species to the core in the form of a low atomic number gas such as CF_4. However, these and other possible studies are beyond the current scope.8

 Early progress was made with deterministic codes that are being used to supplement current MCNP analysis to reduce uncertainties in the neutron dynamics. This effort has proceeded to setup deterministic modeling of the reactor using the 3D discrete ordinates transport code, DOORS3.2. This is to complement some of the Monte Carlo modeling performed earlier and in the present simulations of Section 9.

The 3D graph in Figure 8 is of a quarter section of the reactor core that for now is assumed to be a $3 \, m^3$ right circular cylinder surrounded by a BeO reflector. The peak in power production is at the axial center of the core over an assumed 2 cm width of high-density fissile gas constituted from the interacting shock waves. The intent here is only to capture what a typical power distribution shape might look like for a generic PMI-GCR shock tube. Thus, in particular, the magnitudes indicated in this plot may vary for a given set of reactor parameters. The relative values however are meaningful and could be used to gauge the power distribution for the 1D simulation results to be presented below in Section 8.
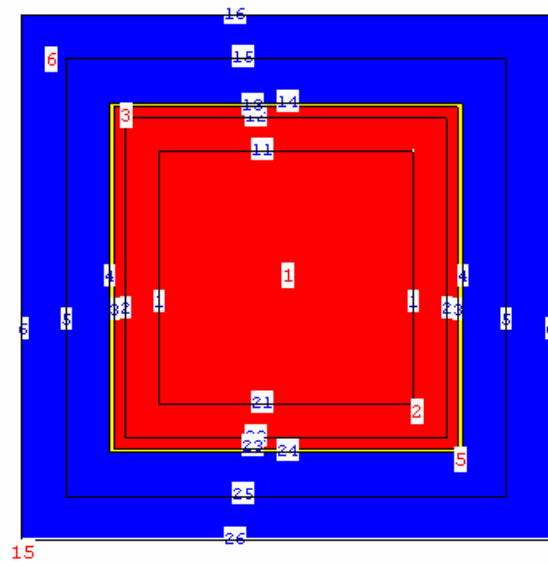
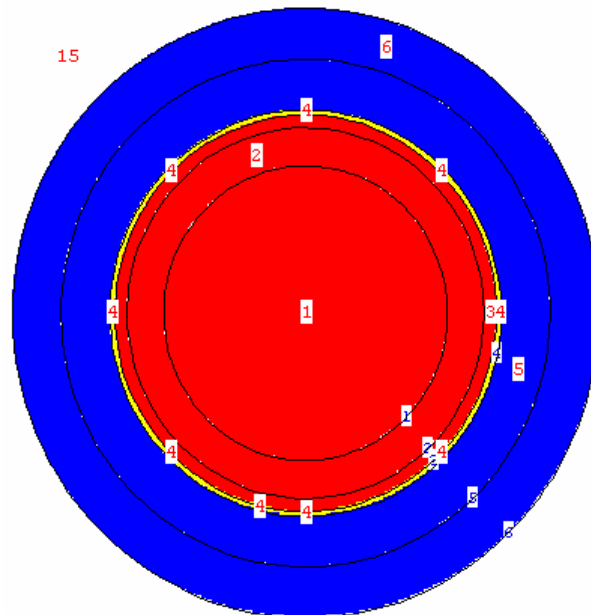Figure 6. Side view of the MCNP model of the simple core and reflector.

Figure 7. Top view of the MCNP model of the simple core and reflector.

A multigroup library was generated for these calculations using ENDF/B-VI neutron data and the NJOY99.81 computer code. This work to produce a set of high temperature multigroup libraries is progressing. We have noted a couple "bugs" in the code as some of the results failed a "sanity check". In particular, NJOY failed to produce realistic multigroup values for $(\nu \sigma_f)$ at low energies. We believe this can be attributed to the fact that these low energies are represented by two constant vectors at these low energies. To provide a temporary fix and produce the attached graph, some hand calculated $\nu \sigma_f$ values for the low energy groups was provided. Current and future work will investigate other codes/methods to work around this problem as additional work is done on producing these libraries.
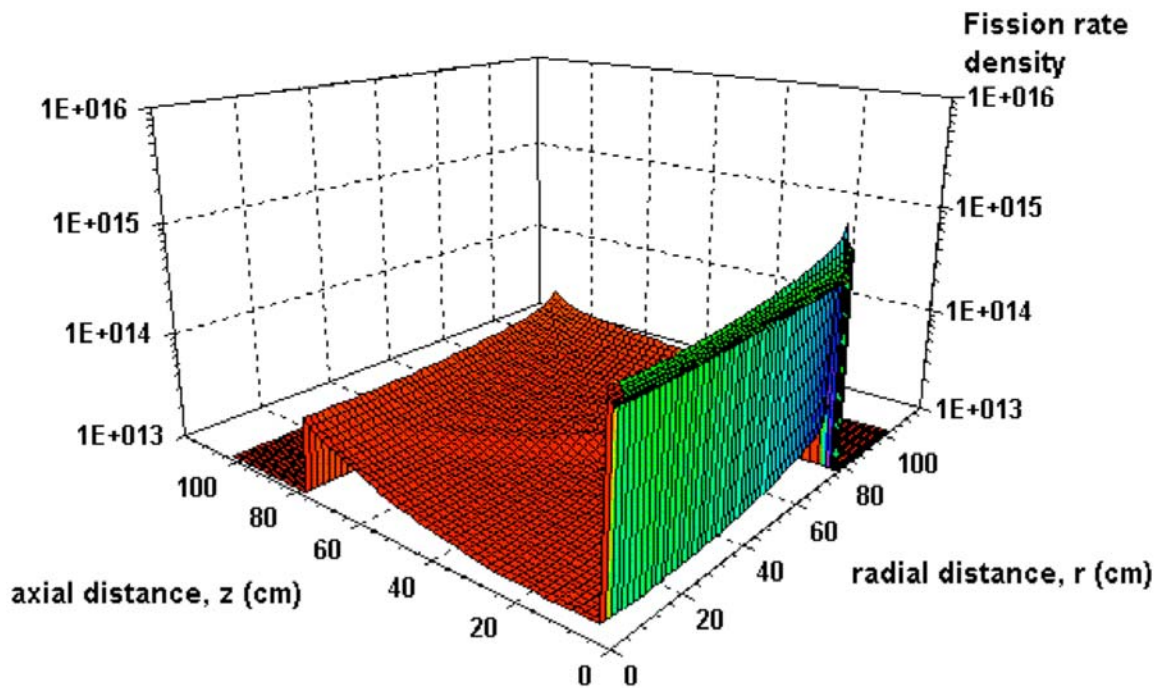
Figure 8. Preliminary results of the fission interaction rate.

The shock tube radius is 80cm, and the moderator thickness 40cm.

The intent is not to show any hard data here, it is only to capture what a typical power distribution shape might look like for a generic PMI-GCR shock tube. Thus in particular the magnitudes indicated in this plot should be ignored. The relative values however are meaningful and could be used to gauge the power distribution for the 1D simulation results to be presented below in Section 8.

8 RESULTS OF THE MHD-MCNP SIMULATION

The results are presented below as three case studies. They have been catalogued by (i) the assumed electrical conductivity $c^2/(\varsigma\, 4\pi)$ of the gas (low or high), (ii) the type of shock generation ("compressor mode" or equivalently "MPD mode" referring to a fixed step current at the boundary that is turned off as soon as the shocks collide in the center of the shock tube, and "pulsed mode" referring to a step current at the boundary that is turned off after a fixed number of time steps), and (iii) various sub-cases depending upon things like shock tube length and/or radius variations, fuel enrichment, initial pressure an density, and so on. In practice the distinction between shock generation methods "compressor" and "pulsed" becomes blurred and indistinguishable when the pulse time is set fairly large and the current density at the boundary is reduced for in that case a pulse becomes almost indistinguishable from a short duration MPD compressor mode. The term "MPD compressor mode" is used because for smaller current densities and longer pulse duration times the shock generation arises mainly from nonlinear wave steepening as described above and in reference [16]. For short pulse times and large current densities the shock generation can be said to arise more from steep magnetic pressure gradient at the boundaries giving rise to shocks from the feedback of magnetic pressure into the gas through classical magnetogasdynamic coupling. There is however a regime where a true pulsed mode could be identified as distinct from a compressor mode by examining the time scales for collisional, relaxation and ionization processes, such an analysis should reveal when the transition from shocked induced gas to induced waves occurs. This report did not look closely at these issues however, so the pulse mode/compressor mode distinction used here to characterize the different studies is somewhat arbitrary.

Before looking at the MHD shock simulations it is instructive to see what happens when two gasdynamic shocks collide.

The main thing to note is that the density sums more or less linearly, as in wave superposition. Some nonlinear effects are evident but viscous dissipation and thermal diffusion spread the shocks out sufficiently for most nonlinear effects to be washed out. In general this is not desirable from a nuclear design point of view because one wants the gas density (number density of fissile atoms) to increase by orders of magnitude to ignite prompt fission supercriticality.

---

[16] C.C. Wu, "Formation, Structure, and Stability of MHD Intermediate Shocks", *J. Geophysical Research*, **95**, No.A6, 8149-81475, 1990.

It appears then that, from the hydrodynamic shock results, the only way to design a useful pulsed reactor would appear to have a strong ambient neutron source placed near the reactor to enhance fission power production in the pulse. We will see that this is the same for fast MHD shocks with one notable difference, the fast MHD shocks will sum nonlinearly when they collide, but most of the energy goes into mechanical pressure in the gas, and the density stays fairly low, although it does increase by a few orders of magnitude, just not enough, *in the absence of a strong background neutron source available for multiplication in the pulse*, for massive (mega-joule) fission power output. This is a somewhat technical distinction that nuclear engineers will be most familiar with, which is to say that subcritical systems are generally designed to achieve high thermal power output *by using an external neutron source* to *boost the total number of fission events*, not to necessarily increase the neutron multiplication factor k_{eff}, which may remain low or at some arbitrary value. The gas does achieve a supercritical state however in the PMI-GCR shock tube simulations, so the basic viability of the concept is proven though not in the way one might have envisaged (one would have expected an intense pulse of power rather than a monotonic increase roughly following the shape of the gas density, see the results below in Sections 8.1 to 8.4.). The remaining question concerns efficiency and practical engineering constraints.
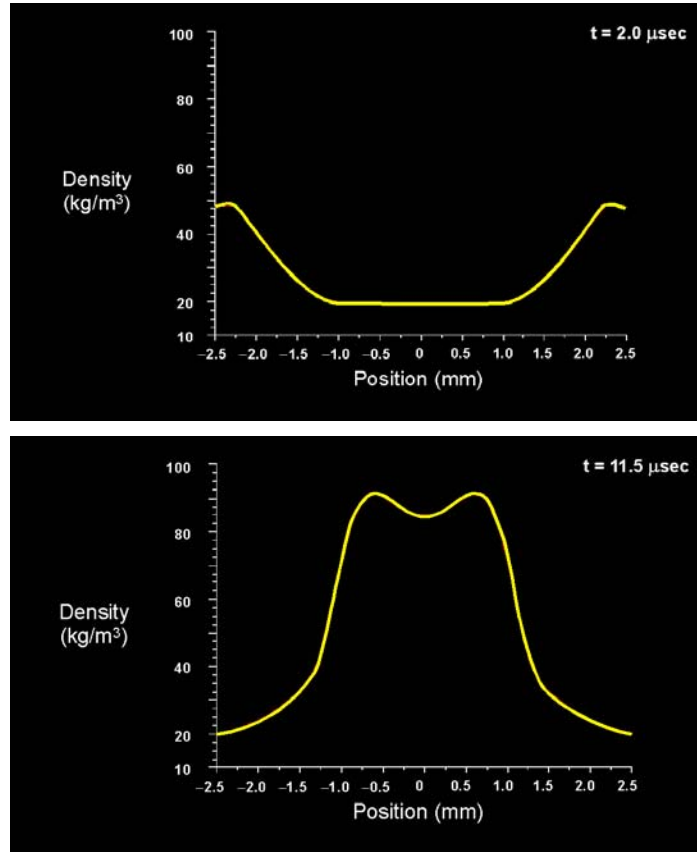
Figure 9. Collision of two hydrodynamic shocks in UF$_4$ gas.

Next, some case studies of various parameter settings and their effect on fission power production and shock collision are presented. The results to follow are obtained by running the MHD1DSHOCK code back-to-back with MCNP4C as described in Section 7.4. The shocks that will now be investigated for the remainder of this report are fast MHD shock waves that carry a strong transverse magnetic field, thus, they are so-called "switch-on" shocks.

For each case study presented, a table is provided showing first the geometry and fuel enrichment, and then the initial conditions and boundary conditions driving the flow (represented by the applied transverse B-field at the boundary and it's pulse time).

8.1   *Case 1–Low Resistivity Plasma, Compressor Mode*

8.1.1   Case 1-a Results, Low Resistivity, Strong Source

The first case here had a 100 cm shock tube length, core radius=80 cm, BeO reflector radius=130 cm, reflector thickness=40 cm. Fuel enrichment=95% 235-U. The resistivity is an almost ideal low 10^{-10} [cm^2.s^{-1}] (in rationalized Gaussian 'cgs'units) throughout. This type of core is a thick pancake shape (diameter exceeds length) and the fission power is large throughout the length due partly to the BeO moderator extending the length of the fuel and beyond. This is perhaps not the best configuration for a well-defined pulse of fission power at the local shock collision region, but with the shock driver in MPD compressor mode and with a strong neutron source, fission power densities of ~7×10^{24} MeV.cm^{-3} or ~1.14 J.m^{-3} were obtained after the shock collision. Neutron flux levels also climbed to 10^{24} n.cm^{-2}.s^{-1}. Although these numbers are impressive one must remember that this case used an irregular core geometry that might not be conducive to realistic shock tube operation. The large diameter to radius has never been used in an electromagnetic shock tube before.

Table 1 Input parameters for Case 1-a.

Core length	Core radius	BeO reflector thickness	Reflector radius	Grid spacing	Fuel enrichment
100 cm	80 cm	40 cm	130 cm	0.167 cm	95%

P_0 [dynne/cm^2]	ρ_0 [g/cm^3]	T_0 [^{o}K]	B_y (right) [Gauss]	Pulse time [ms] (approx.)	Source [n per s]
10^7	0.024	1567	+708	1.1	10^{15}

Frames taken from the time evolution of this simulation are shown over the page for gas density, fission power density and neutron flux. The results seem somewhat counterintuitive in many respects. In particular the gas density peaks when the shocks collide but then only very weak outgoing density waves are reflected. The pressure and temperature for the outgoing waves are not extremely high—the temperature reaches a peak of 3500°K, but this is without the massive heat generation from the fission power source added to the MHD equations. So in actuality one would expect extreme fission heating of the gas and a very strong outgoing blast wave that would almost completely ionize the UF4 gas mixture. This is perfect for conversion to electrical power with a MFCG or other inductive circuit. Nevertheless, even with the fission heating source term uncoupled, the behavior of the pure MHD shock collision is curious and interesting. One thing should be noted, which is that the way the shock driver is set up the shock tube must have a make-up supply of gas fuel in order for fluid to be compressed and built up in the core. In other words, the MPD compressor river sucks in (or pushes in) a huge amount of gas during the simulation (i.e. mass is certainly not conserved within the simulation control volume, or more exactly, *total control volume fluid mass is not a constant during the simulation* because of the large (real) mass flux across the boundaries). There is a huge pressure built up that does not allow the gas to escape rapidly. It may be possible to somehow engineer the system to recover a more classical shock collision and reflection, but without the fission heating coupled to the MHD equations it is premature to speculate upon what might be the most favorable configuration.

The fission power density follows the spike in gas density only weakly and is otherwise fairly uniform throughout the core. This can be understood because of the large effect of the reflector. The mean free path of the fast neutrons born in the reactor is long because of the relatively low density in the core compared with condensed matter. Many such neutrons that leak into the reflector slow down in energy before being scattered back to the core. These thermal or nearly thermal neutrons have much shorter mean free paths and experience absorption or fission largely in areas near the walls of the shock tube. Since the current simulation is one-dimensional this radial dependency is averaged out. What is observed is the larger amount of fissions occurring in the shockwave because of its greater density of fissile material and neutron flux but also to a lesser degree in adjacent cells since these are in proximity to the same thermal neutrons emerging from the reflector. This explains the somewhat broadened peak in fission heating.

Also noticeable is the fact that the fission power and neutron flux continually increase as time advances following the shock interaction. This again is explained by the huge amount of fluid that is transported into the tube and compressed by the boundary current and transverse magnetic field pressure.

The fission power density axial (x-coordinate) spatial variation follows the gas density roughly, though it is smeared out somewhat. The neutron flux appears quite flat however. This is quite natural. What is plotted in the case of the neutron flux below is the integrated neutron flux over all neutron energies. Referring back to Figure 8 in the previous section, one can see the axial and radial dependence of the fission power density for a mock-up of a shock collision profile. In that figure one can readily reinterpret the vertical axis as the thermal neutron flux instead, because the power density correlates most strongly with the distribution of thermalized neutrons. The GCR is not a pure fast or slow reactor in this sense, the power is produced by both fast and slow neutrons, but clearly the thermal neutrons dominate in fission power production. In the *integrated neutron flux* plots recorded below one sees the effect of both fast and slow neutrons on the total neutron flux, and this is clearly almost dead flat across the shock tube, because fast neutrons are generated throughout the gas fuel and are reflected back into the gas uniformly as well. The reason the power density doesn't appear so flat is because fission events, on average, occur preferentially near the reflector, i.e. in the gas near the walls where thermal neutrons reenter, and also near the highest density regions near the shock waves. The mean free path of the fast neutrons in the gas fuel is so large that fast neutrons don't really see the variation in gas density. This explains why the integrated neutron flux is so flat.

The UF4 gas pressure is plotted after the series of neutron flux plots for the same time frames as the gas density and fission power density. One can see the rise in gas pressure that follows the shocks. However it is clearly not the mechanical pressure alone that prevents most of the mass escaping with the outgoing reflected shock fronts.

Following the series of pressure plots, one can see the same time frame variation in the transverse magnetic field that travels with the shock waves. The By component increases to a large magnitude and also spikes as the shocks collide. After collision however the rise in the By is sustained, but more importantly it is propagated along with the outgoing reflected shock fronts that are weaker than the incoming shock fronts. Nevertheless, this strong magnetic field exerts considerable pressure on the ionized gas; this explains why the pocket of high-density gas remains in the center of the shock tube.

The gas temperature is also increased by the shock collision; this will raise the electrical conductivity of the gas and help to create the same high magnetic pressure. For a realistically high resistivity UF4 plasma (with little or no seed material to boos conductivity) there is good reason to expect that even for realistic partial plasma or weakly ionized gas models the same effect will occur.

42

Case 1-a time frames: Low Resistivity Plasma, Strong Source, BeO End Wall.
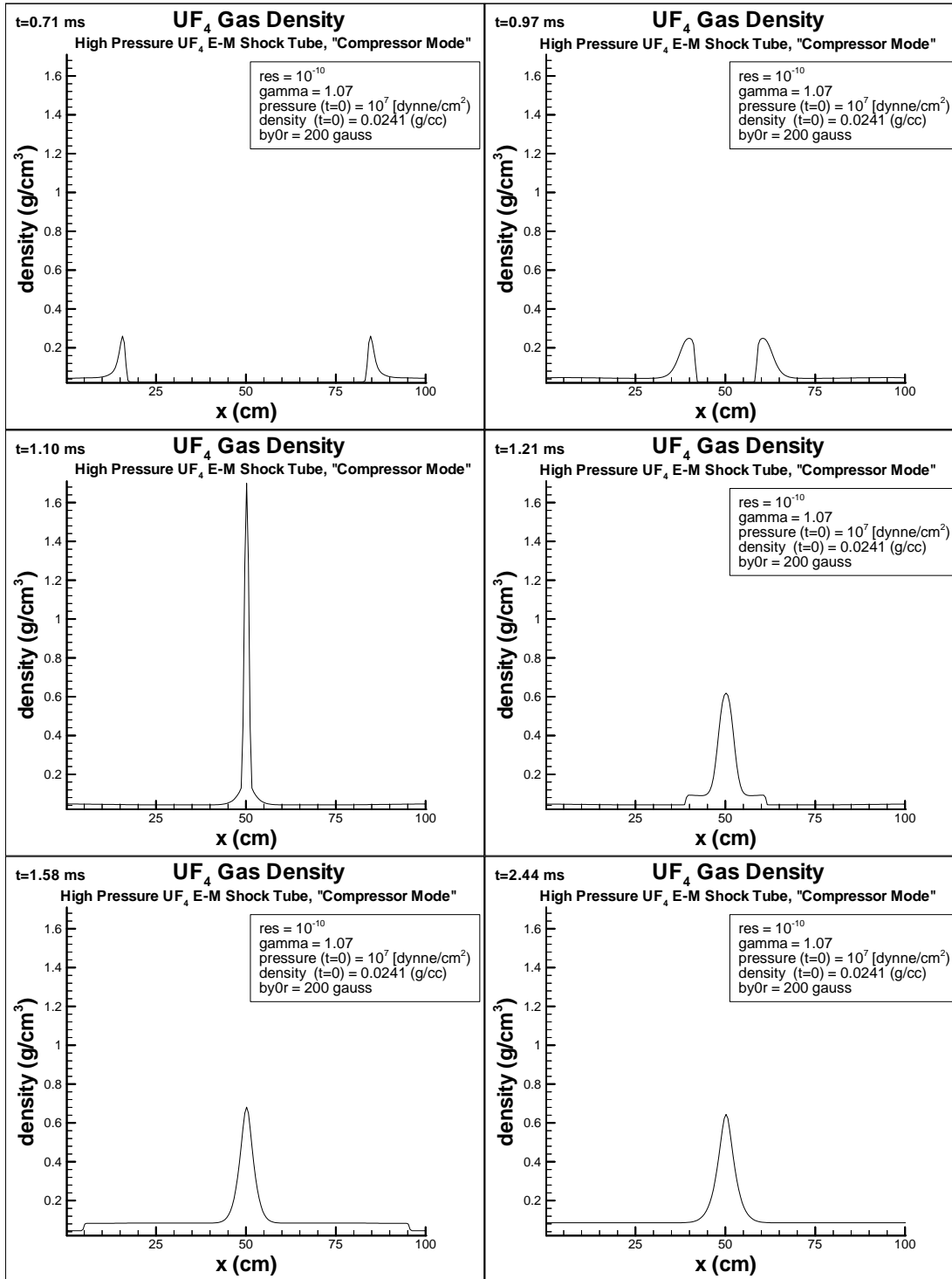
Case 1-a Fission Power Density, for the same time frames.
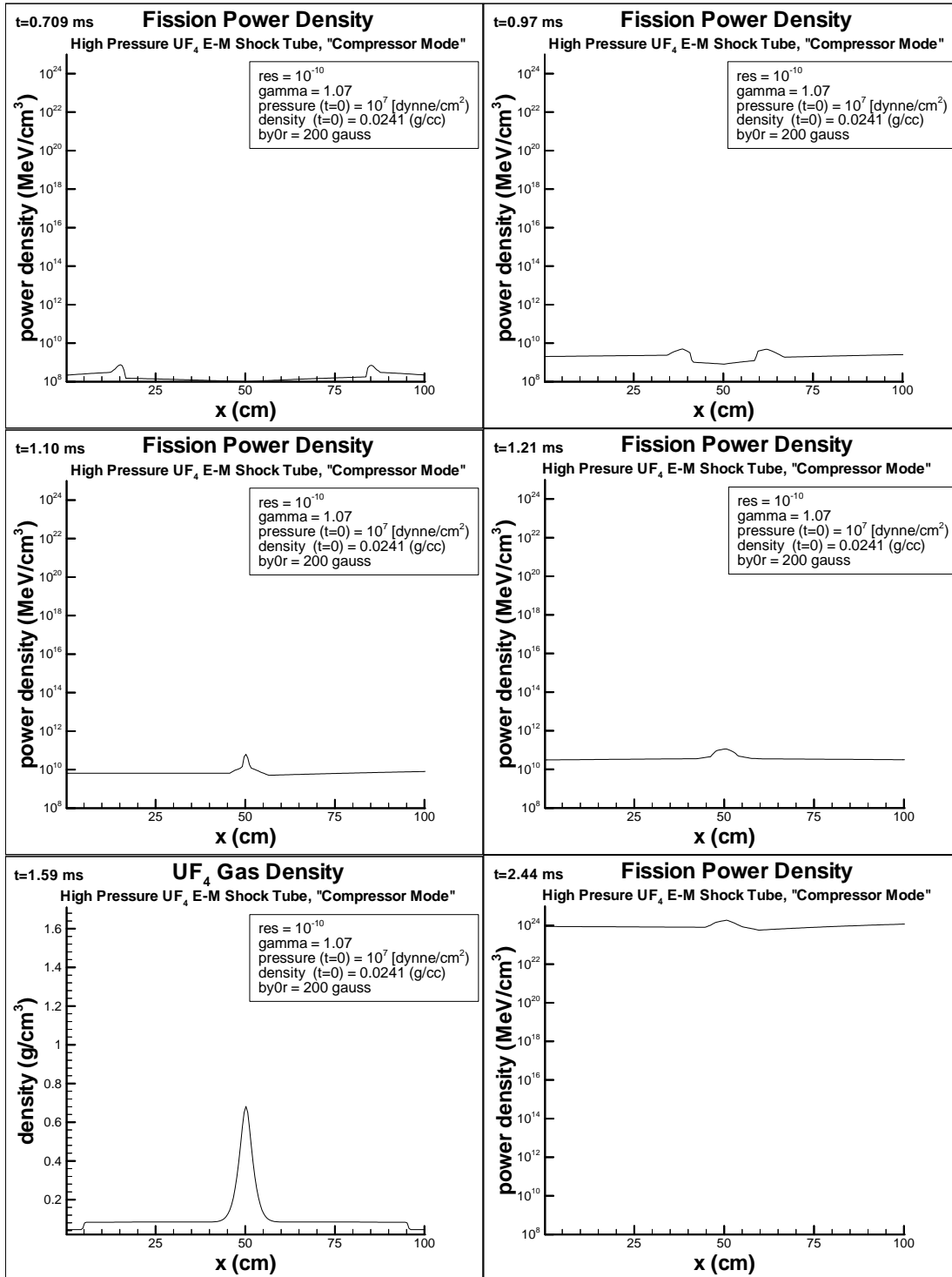
Case 1-a *Integrated* Neutron Flux, for the same time frames.

Case 1-a UF$_4$ Gas Pressure, for the same time frames.
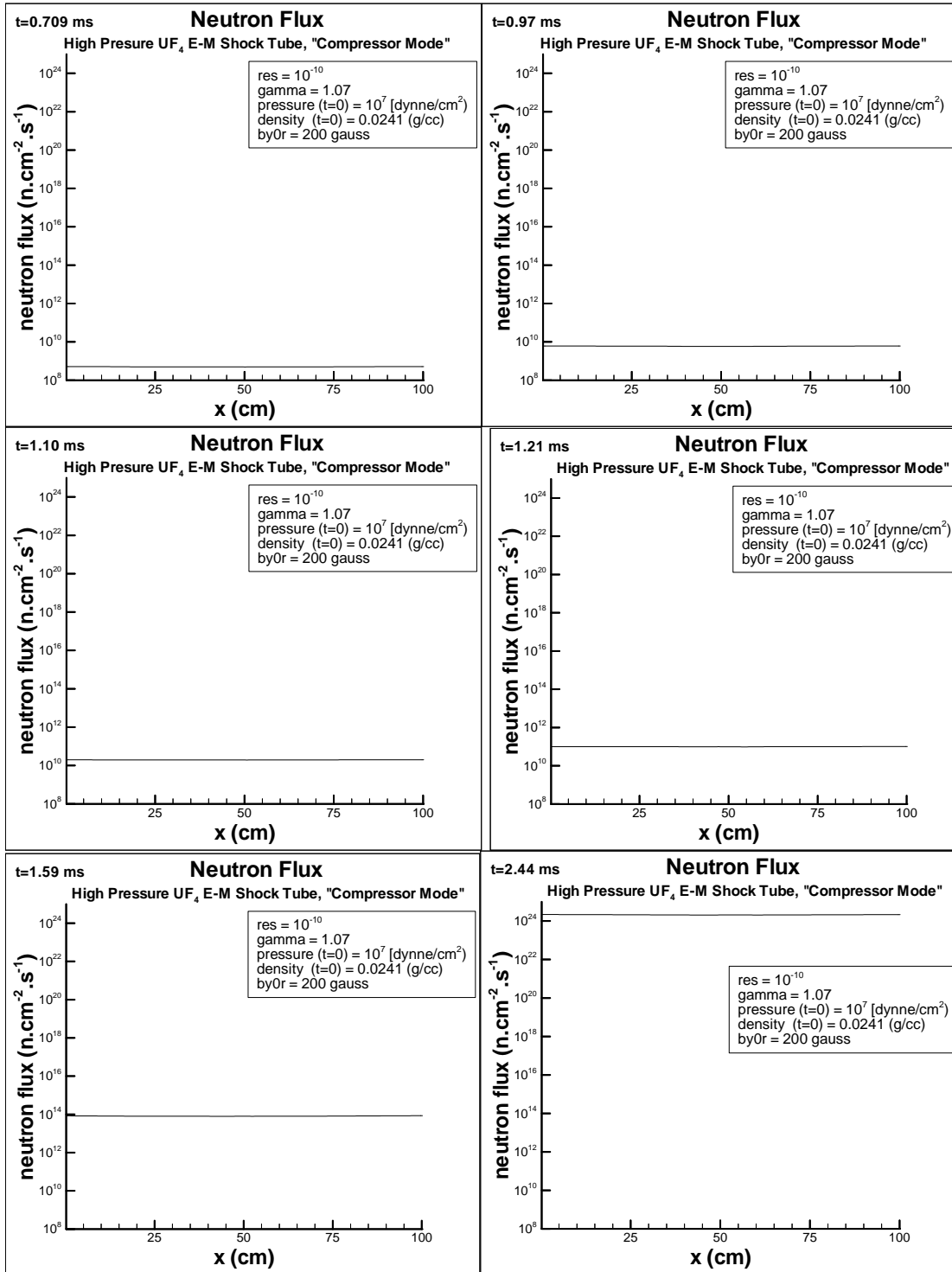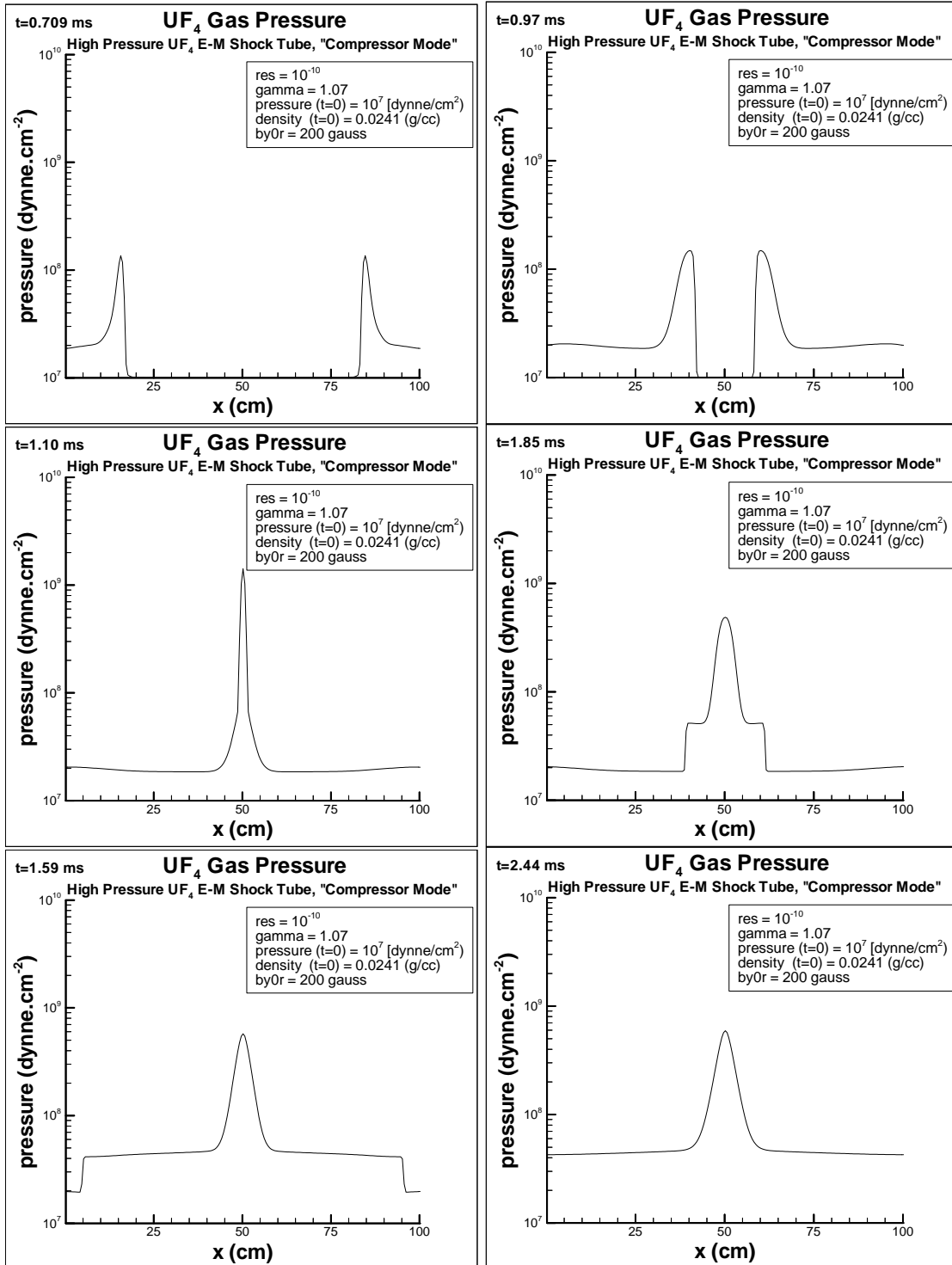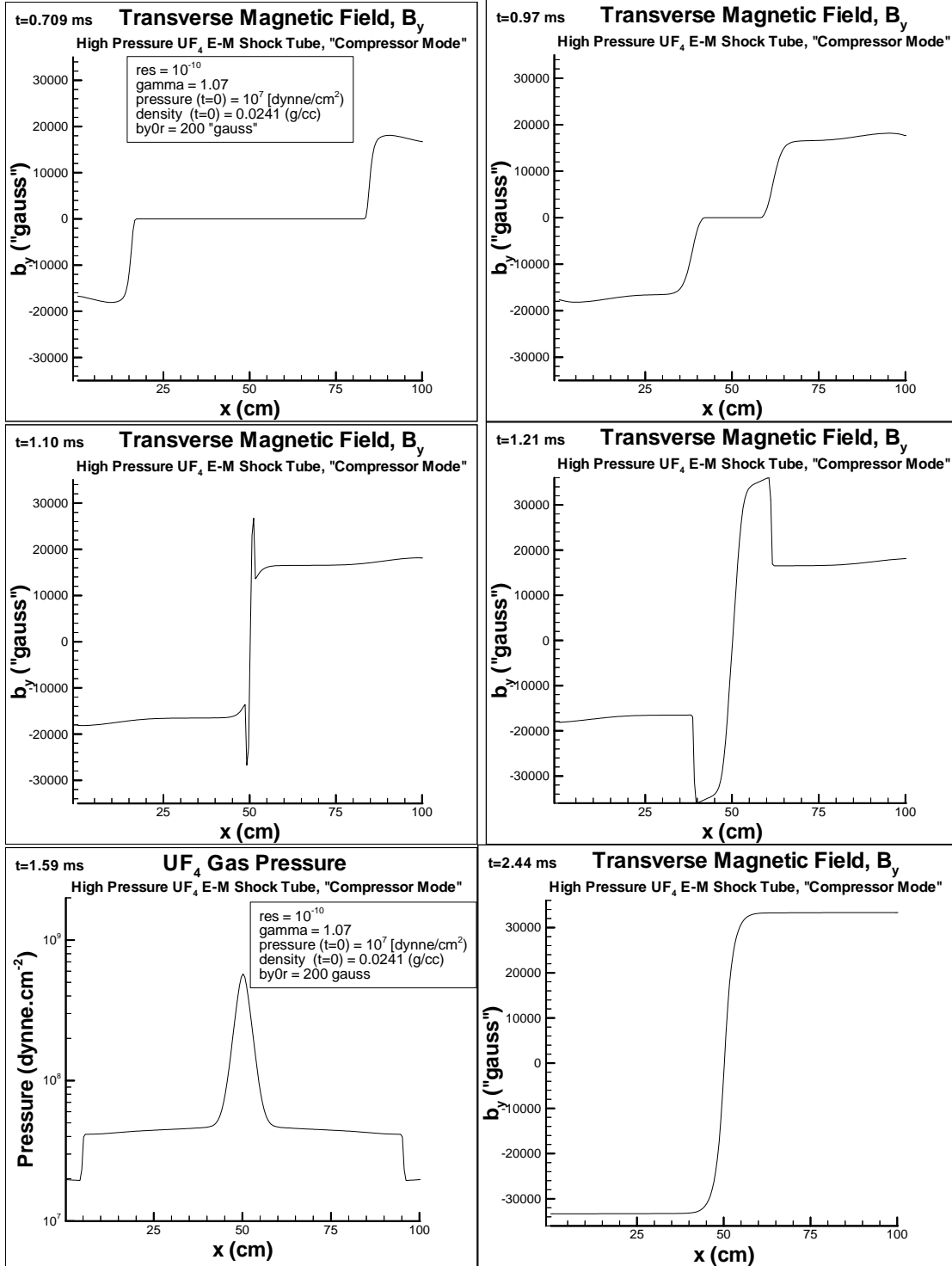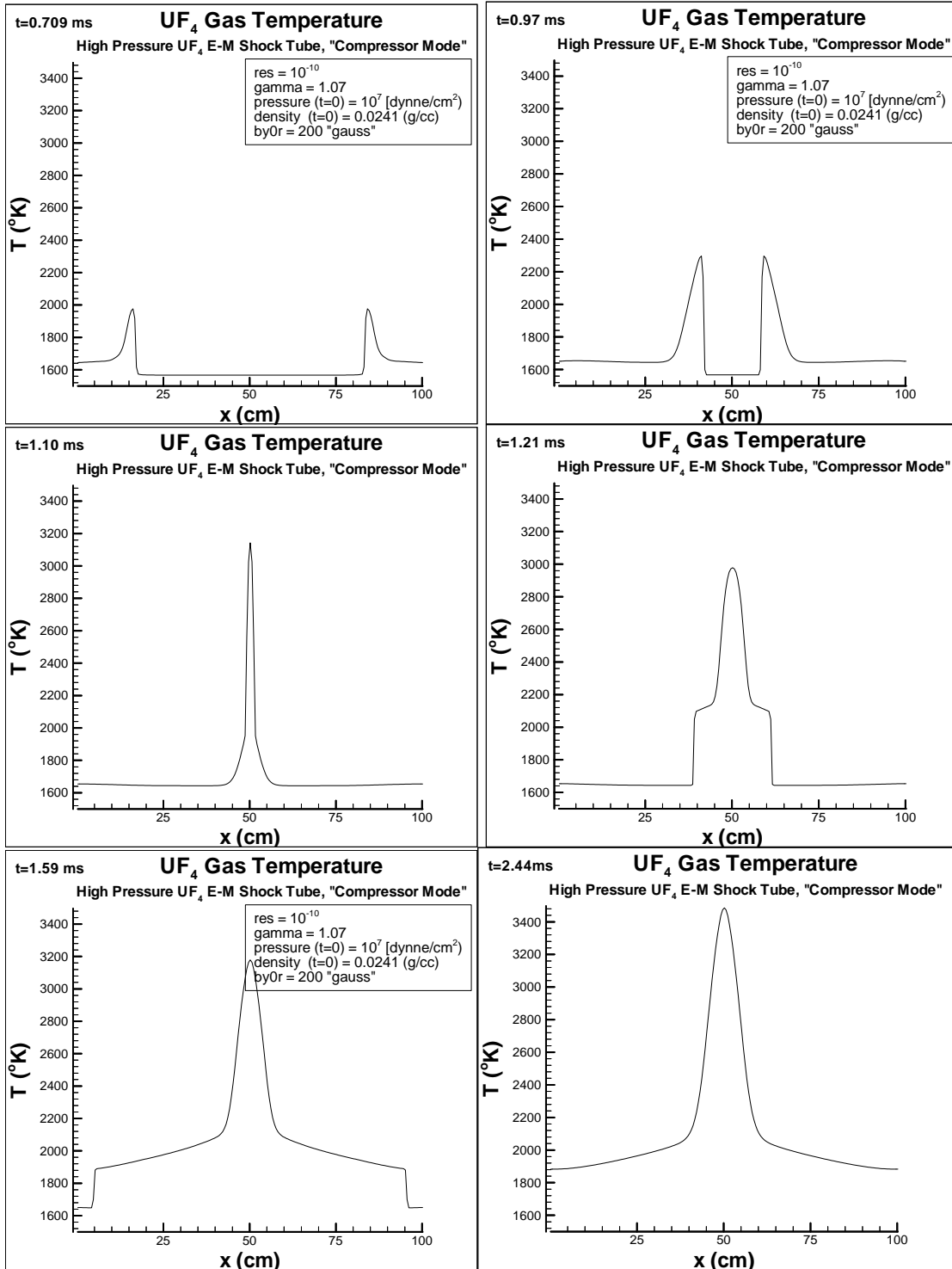

46

Case 1-a Transverse Magnetic Field ($b_y = B_y[\text{Gauss}]/\sqrt{4\pi}$), for the same time frames.

Case 1-a UF$_4$ Gas Temperature, for the same time frames.

Case 2–High Resistivity Plasma, Compressor Mode

In this case much higher resistivity plasma was chosen, this would simulate a weakly ionized gas. Although not very realistic (because the intense shock waves can almost completely ionize a gas at the shock front) this does give one an idea of how a non-ideal working fluid behaves. This example is slightly atypical in that the grid cell size was coarsened considerably to 1.0cm in order to avoid negative pressures forming at the grid boundary. A fairly strong applied magnetic field was required to get sizeable densities at the shock collision.

8.2.1   Case 2-b Results, High Resistivity, Strong Source

Input parameters used are summarized in Table 2. Results are plotted for a few time frames over the page. The resistivity is 10^5 [cm^2.s^{-1}] throughout.

Table 2. Input parameters for Case 2-b.

Core length	Core radius	BeO reflector thickness	Reflector radius	Grid spacing	Fuel enrichment
100 cm	50 cm	40 cm	100 cm	0.167 cm	95%

P_0 [dynne/cm^2]	ρ_0 [g/cm^3]	T_0 [$^\circ$K]	B_y (right) [Gauss]	Pulse time [ms] (approx.)	Source [n per s]
10^7	0.024	1567	+35450	0.10	10^{15}

The most noticeable difference between this case and the low resistivity plasma (Case 1-a) is the speed of the shock. This is produced by the larger applied magnetic field (note that *by*0r=10000 "gauss" in the figures actually corresponds to a real applied magnetic intensity of $B_y = by0\sqrt{4\pi}$ [Gauss] =35450 Gauss). The fission power density is lower, partly because the neutron population did not have sufficient time to build-up to significant numbers. However, there was still a large fission power release, though probably not enough for a big power gain.

Case 2-b time frames: High Resistivity Plasma, Strong Source, BeO End Wall.

Fission Power Density
t=0.144 ms
High Presure UF$_4$ E-M Shock Tube, "Compressor Mode"

res = 10^5
gamma = 1.07
pressure (t=0) = 10^7 [dynne/cm^2]
density (t=0) = 0.0241 (g/cc)
by0r = 1000 gauss

power density (MeV/cm^3)

x (cm)

Fission Power Density
t=0.211 ms
High Presure UF$_4$ E-M Shock Tube, "Compressor Mode"

res = 10^5
gamma = 1.07
pressure (t=0) = 10^7 [dynne/cm^2]
density (t=0) = 0.0241 (g/cc)
by0r = 1000 gauss

power density (MeV/cm^3)

x (cm)
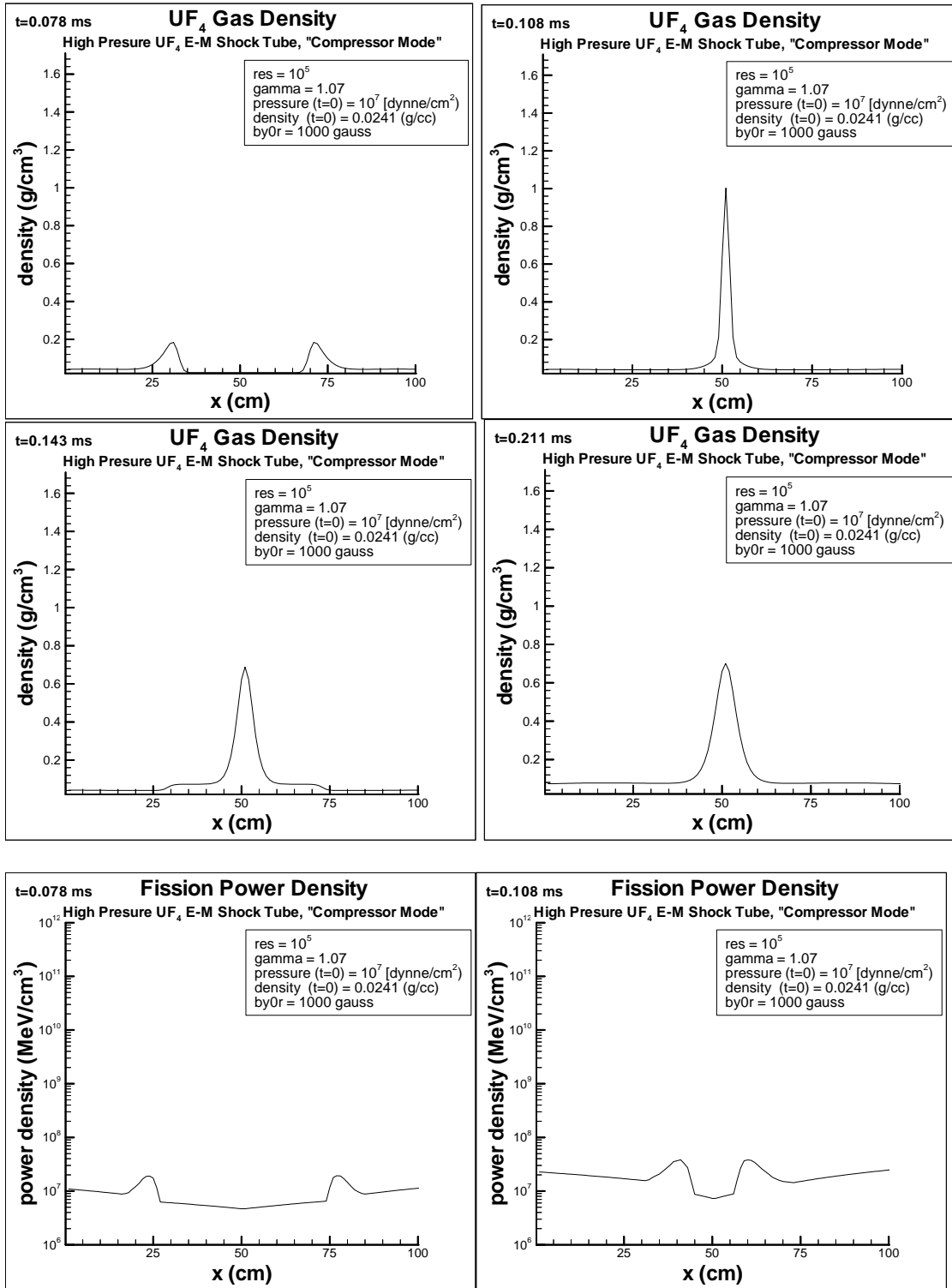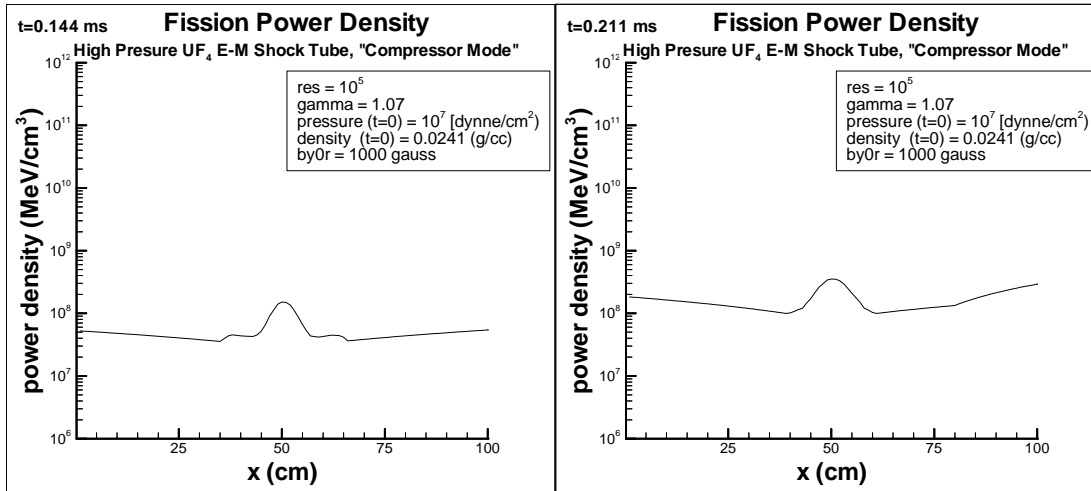
As with Case 1-a the density stays large in the middle of the shock tube. The other difference in this case is that the reactor is smaller; it is a right cylinder of diameter 100 cm. So there is less fuel to begin with in Case 2-b here. The neutron source strength was the same and the moderator dimensions the same as Case 1-a, so Case 2-b suffers from smaller reactor size and overly rapid shock collision.

The moderator material at the ends of the shock tube gives a pronounced higher fission power density near the end boundaries, although the power rise still follows the variation in density fairly closely. For this simulation the fission power continues to rise throughout the reactor as time goes by and rises to about 4×10^{18} MeV.cm^{-3} after 1.60 ms, which is considerably higher than the power released at the moment of greatest density. Moreover the trend indicates that the power would continue to climb, so there appears to be almost enough mass now in the shock tube to generate a run-away surge as happened in Case 1-a. This is an effect of the quasi-steady density pile-up in the shock tube that has forced so much fuel mass into the moderated region. This points to the need to engineer some kind of fuel dispersal after the shock collision (only if the fission heat source doesn't achieve a blow-away of all the mass, which one would probably expect!).

Case 3–Moderate Resistivity Plasma, Compressor Mode

8.3.1 Case 3-a Results, High Resistivity, Long Pulse Duration, Strong Source

For this case a time in seconds was used to control the applied field drive time, thus in the input table the pulse time is marked as exactly 0.1 milli-seconds. Other parameters are typical of those used elsewhere, though the source strength was moderate at 10^{12} n/sec. The fission power is plotted in units of MeV/cm^3. This shock tube was surrounded by a BeO annulus reflector and had 40 cm thick structural material (Zr) as the end walls, so the overall length was 280 cm. The resistivity is 1.0 [cm^2.s^{-1}] throughout.

Table 3. Input parameters for Case 3-a.

Core length	Core radius	BeO reflector width	Reflector radius	Grid spacing	Fuel enrichment
200 cm	60 cm	200 cm	110 cm	0.2 cm	95%

P_0 [dynne/cm^2]	ρ_0 [g/cm^3]	T_0 [$^{\circ}$K]	B_y (right) [Gauss]	Pulse time [ms] (exact)	Source [n per s]
10^7	0.024	1567	+7090	**0.1**	10^{12}

In this simulation the fission power again gradually increases monotonically throughout the reactor shock tube core, it climbs reasonably steadily to ~3×10^{16} MeV.cm^{-3} after 2.1 ms, and shows no sign of decreasing.

Accompanying the plots of the gas density is a time history of the neutron scale factor (number of neutrons) used by the nuclear code to normalize statistics. Over the page are the corresponding plots of the fission power density.

Case 3-a time frames: Moderate Resistivity, Long Pulse Compression, Moderate Source, Zr End Wall.

(a) UF$_4$ density.

Neutron Population vs Time

High Pressure UF$_4$ E-M Shock Tube, "CompressorMode"

res = 1.0
gamma = 1.07
pressure (t=0) = 10^7 [dynne/cm^2]
density (t=0) = 0.0241 (g/cc)
by0r = 2000 gauss
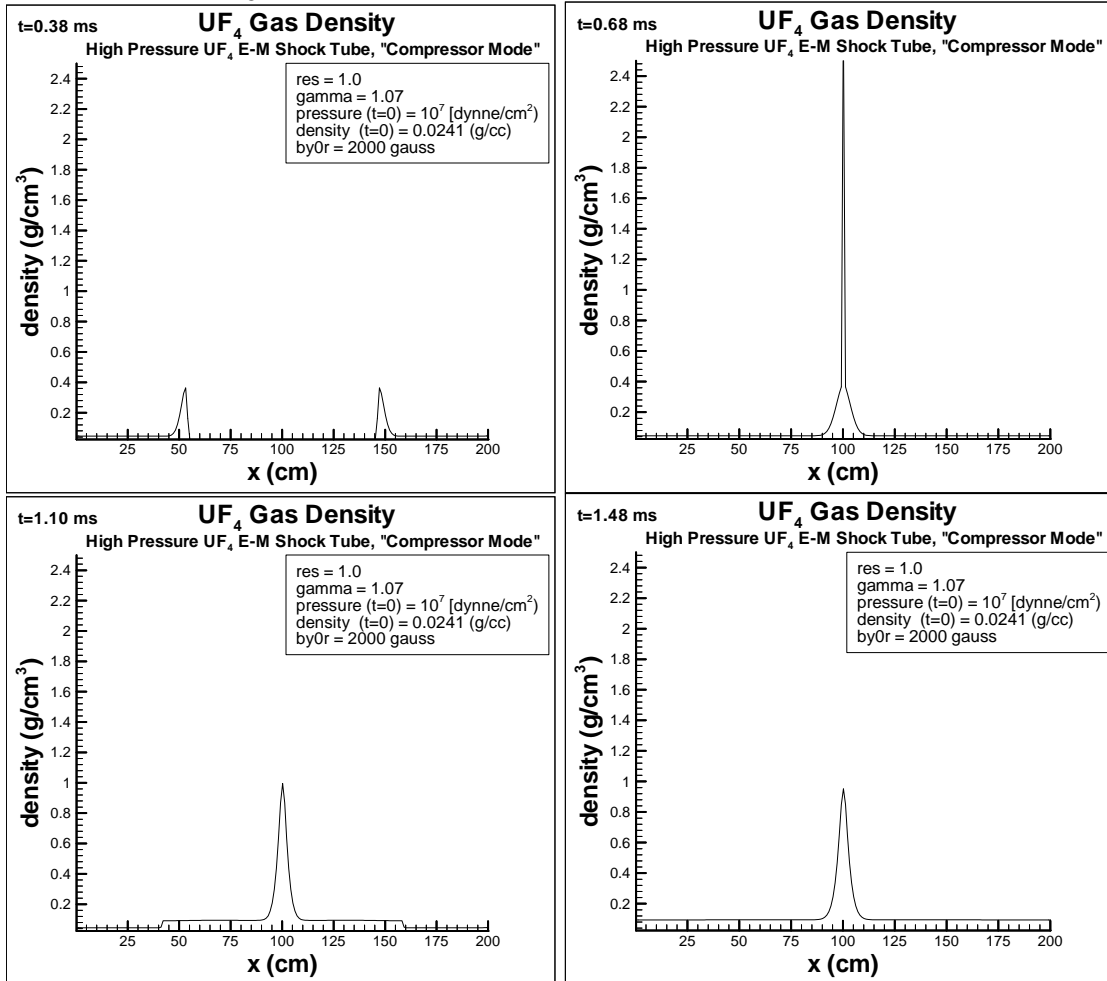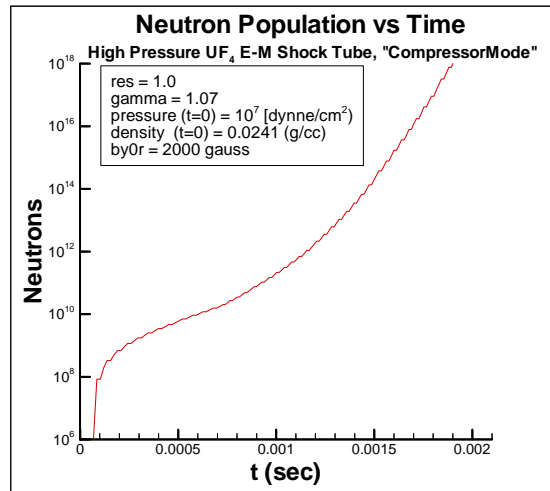
Figure 10. Neutron population versus time for the long duration pulse (Case 3-a).

(b) Fission power density.

Four plots of Fission Power Density: "High Pressure UF₄ E-M Shock Tube, 'Compressor Mode'" at t=0.38 ms, t=0.68 ms, t=1.10 ms, and t=1.48 ms. Each shows power density (MeV/cm³) versus x (cm), with parameters res = 1.0, gamma = 1.07, pressure (t=0) = 10⁷ [dynne/cm²], density (t=0) = 0.0241 (g/cc), by0r = 2000 gauss.
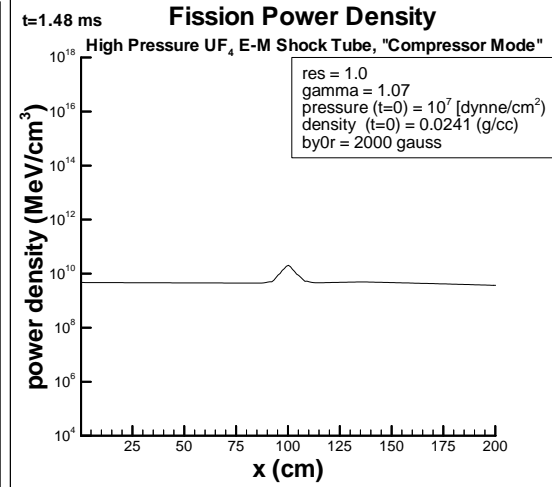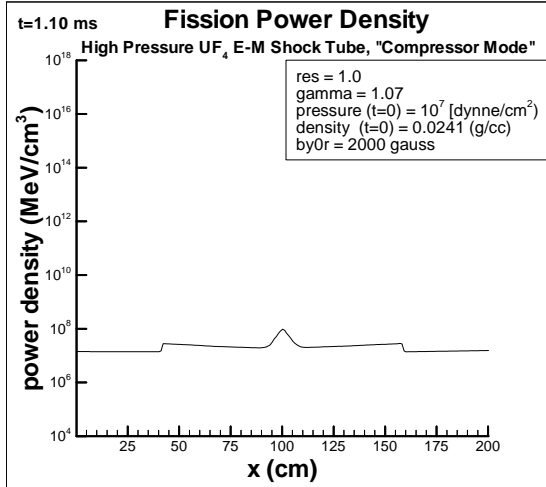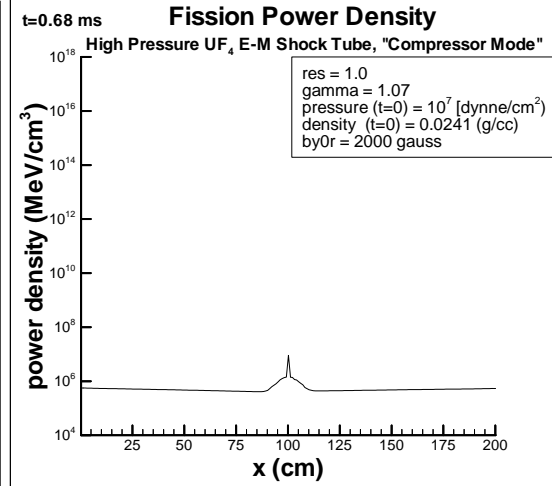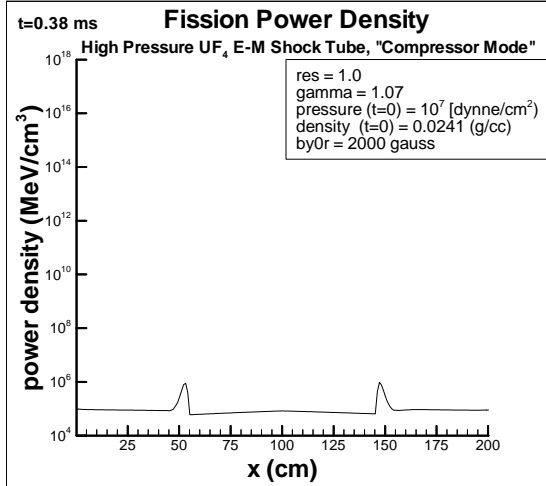
8.4 *Case 4–High Resistivity Plasma, Pulsed Mode*

For this study the applied magnetic field representing the shock generating current density and ponderomotive force was reduced in duration.

8.4.1 Case 4-b Results, High Resistivity, Pulsed Mode, Strong Source, BeO End walls

For this case we plot the fission power in units of MeV/g, and place the plots next to the corresponding density at the same time. So density is on the left with specific fission power on the right. For the input parameters notice the pulse time here of only 0.02 ms. The core has a fairly large radius=80 cm to get slightly more fuel mass initially in the core to compensate for the lower drive power. This shock tube was entirely surrounded by 40 cm thick BeO moderator.

Table 4. Input parameters for Case 4-b.

Core length	Core radius	BeO reflector thickness	Reflector radius	Grid spacing	Fuel enrichment
100 cm	80 cm	40 cm	130 cm	0.167 cm	95%

P_0 [dynne/cm^2]	ρ_0 [g/cm^3]	T_0 [^{o}K]	B_y (right) [Gauss]	Pulse time [ms] (approx.)	Source [n per s]
10^7	0.024	1567	+35450	**0.02**	10^{15}

The results are not dissimilar to the compressor mode studies. Remember that now the specific power is plotted. If the power density was plotted then the results would look very much like the history in Cases 1-a and 2-b, only different characteristic times and power magnitudes are involved.

Notice that this means the core (shock tube) is quite pancake shaped, (diameter exceeds length). This helps get more mass into the core at high density while limiting dissipation of the shock. However it looks as though the shocks do not significantly dissipate, nor would they be expected, given the absence of viscous and heat radiation or conduction losses in the governing equations. In future simulations however it may prove that a real (viscous weakly ionized) gas will produce rapidly attenuated shocks that weaken into linear waves and fail to produce high density in the reactor. Such effects might not result in loss of power, however, if run in MPD compressor mode, because as the Cases 1 and 2 show, one doesn't necessarily need supercritical densities in confined regions to generate lots of power, a smeared out shock or sum of waves might do just as well (ignoring for the present time issues of power extraction, that is).

Case 4-b time frames, Pulsed Mode, High Resistivity, density and q_{fiss} plots.
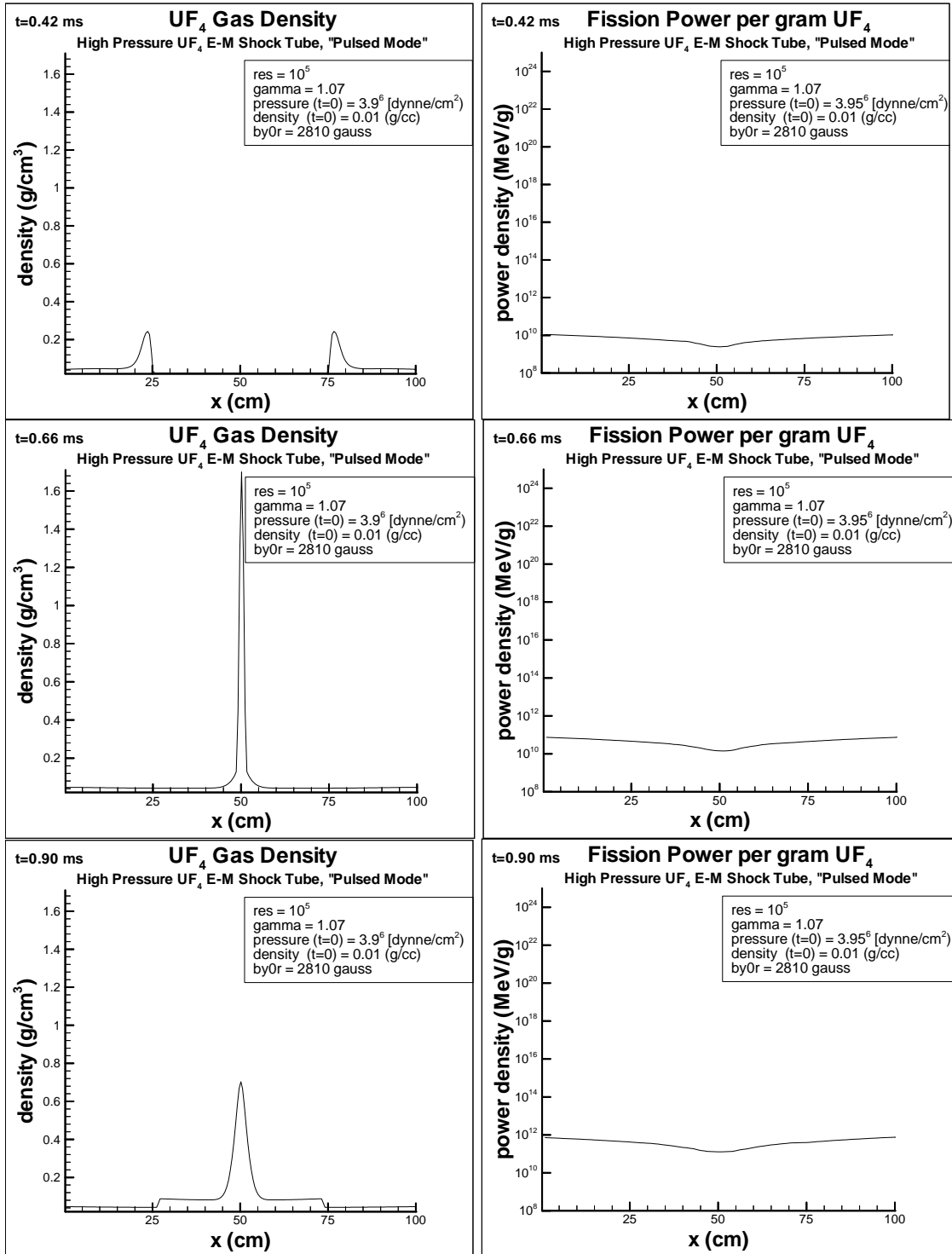
Case 4-d Results: High Resistivity, Pulsed Mode, Medium Source, Zr End Wall

Another trial with weaker neutron source strength was simulated. This time with 40 cm thick Zr structural walls at the ends of the tube. The shock tube was made fairly large to compensate, and the applied magnetic field was increased slightly to about 21300 Gauss, but the pulse duration was extremely short, only 5.0 microseconds. For this case we again plot the fission power in units of MeV/g, and place the plots next to the corresponding density at the same time.

Table 5. Input parameters for Case 4-b.

Core length	Core radius	BeO reflector thickness	Reflector radius	Grid spacing	Fuel enrichment
200 cm	80 cm	50 cm	130 cm	0.5 cm	95%

P_0 [dynne/cm^2]	ρ_0 [g/cm^3]	T_0 [$^{\circ}$K]	B_y (right) [Gauss]	Pulse time (approx.)	Source [n per s]
10^7	0.024	1567	+21 300	**5.0 μs**	10^{12}

The waves are no longer acting nonlinearly and they are fairly weak. One would expect that megagauss fields would be needed to produce strong shock waves with such short applied field pulse duration, and this is indeed what these results seem to indicate. Figure 11 shows the neutron population as a function of time.
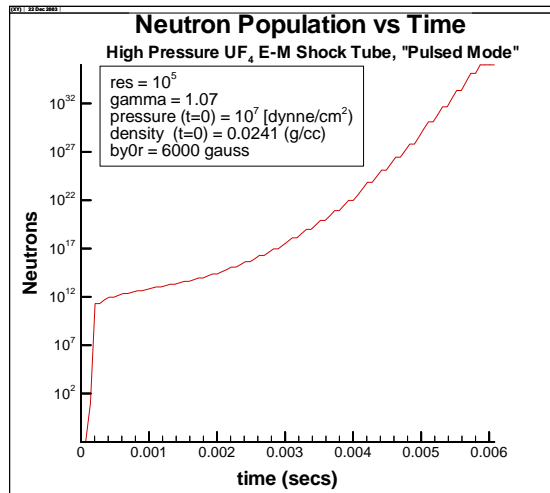
Figure 11. Neutron population versus time for the short pulse trail (Case 4-d).

The curious thing is that here we see that even for a long time period after shock collision the mass of fissile fuel dragged into the shock tube confines can eventually lead to a huge multiplication of the ambient background neutron population. Thus, fission energy is eventually released, just not as violently, nor perhaps as usefully, as might occur in a classic shock collision followed by reflection.

Case 4-b time frames: Microsecond Pulsed Mode, High Resistivity, density and q_{fiss} plots.
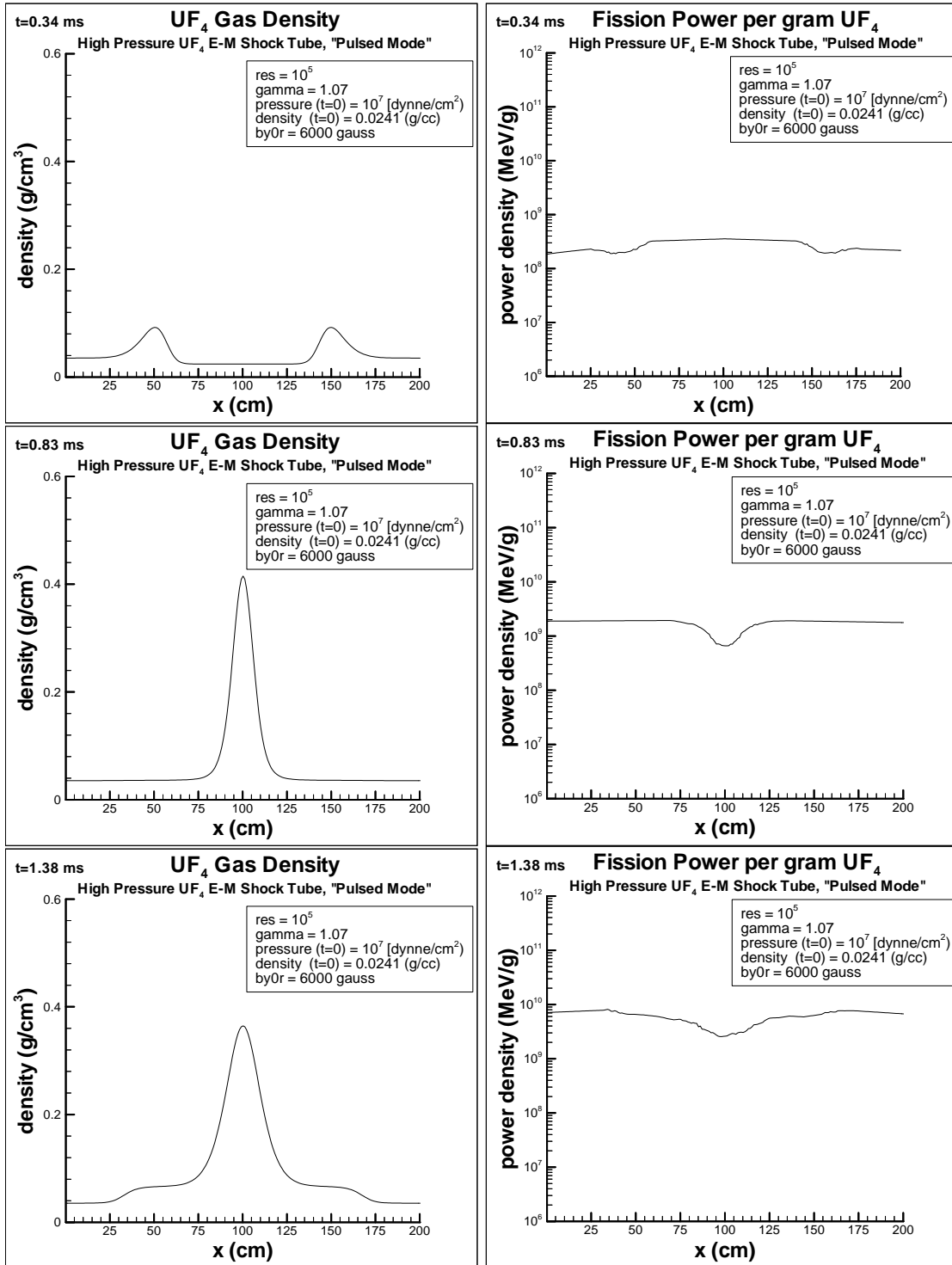
Other Case Studies

A whole series of trials with various input parameters has been under investigation to systematically search for an optimum configuration of geometry and shock generator that can maximize the peak density and lead to high fission power density during shock collision. This is the time at which one wants fission energy to peak so that power can be extracted from the explosive effect on the ionized gas. However, to date although most trials eventually are found to result in a build-up in neutrons and consequent monotonic increase in fission power output, efforts are still on-going in finding either a classical shock collision and reflection regime with sudden fission energy burst, or to find a regime where the fission energy at least spikes momentarily as the shocks collide.

There are so many parameters controlling the PMI-GCR shock wave driven system that it is prudent to avoid speculating upon all the possible avenues open for improving upon the research presented in this report, or this report would become a behemoth. Take just one example, if the persistent build-up of fluid in the shock tube is a real effect then it offers alternative ways to design a power conversion device from this concept. Perhaps one can even start with a very rarified low density, low pressure fluid and still get massive quantities of fission energy over slightly longer time intervals, merely by electromagnetically compressing the fluid. Such case studies await future endeavors and may even constitute a totally new class of competing shock driven reactors.

9 SUMMARY, CONCLUSIONS AND RECOMMENDATIONS

9.1 **Summary of Research Findings**

It has been seen that pure hydroshocks in UF_4 dissipate too rapidly for nonlinear increases in the gas density required for effective fission power production. With fast MHD shocks however it was shown that waves can be formed that steepen into shocks that sum highly nonlinearly, but with most energy locked up in mechanical pressure, although the plasma density does increase by orders of magnitude as well, only not as greatly as the hydrostatic pressure. Yet this may not be enough to achieve a highly supercritical core that would be necessary for massive ($\sim$ MJ/cm^3) fission energy output. The gas does achieve a supercritical state however, so the basic viability of the concept is proven. There is certain potential for extraction of net power from the PMI-GCR system. The remaining question concerns efficiency and practical engineering constraints. In further simulations, release of hundreds of thousands of Joules over a few microseconds is possible through the introduction of a strong neutron source for significant fission power through multiplication in the pulse due to the shocktube prompt critical state afforded by the nonlinear increase in density.

The recommended gross design parameters that emerge form the research so far, for a viable PMI-GCR power supply, are listed in Table 6.

Table 6. Recommended design parameters for an ambient-subcritical electromagnetic shock-driven PMI-GCR.

Core radius	>80cm
Shock tube length	200cm
Moderator thickness	50cm
^{235}U enrichment	95%
Neutron source	10^{10}–10^{15} n·sec^{-1}
Ambient gas pressure	1 MPa
Ambient gas density	0.024 g·cm^{-3}
B-field strength (MPD mode)	0.2 to 3.0 Tesla
B-field strength (pulsed mode)	20 to 200 Tesla

Comparison of results for Case 1 and Case 2 shows that higher resistivity partial plasma reduces the effectiveness of fission power production (although only indirectly through the shock collision effects). It may be that the gas conductivity used for Cases 2 and 4, $\varsigma = 10^{-5}$ [cm^{-2}.s] is too low and not representative of the conductivity that a shock heated gas might approach. Undoubtedly more investigation needs to be done to ascertain whether or not the reactor parameters recommended here will yield orders of magnitude lower or higher fission power production. One can only conclude that the reactor is viable and that there is a highly novel and interesting phenomenon that occurs leading to sustained accumulation of fuel mass in the center region of the electromagnetic shock tube, this critical mass allows sustained growth in the neutron population and hence in the fission power yield over many milliseconds. So far simulations have not looked forward far enough in time to see if this dynamic effect is sustainable. So the PMI-GCR concept is both intriguing and worrisome. It is not yet known whether it can be made efficient and practical. That is, one cannot yet say whether the system will perform as a useful power supply even though under the high magnetic field compression performed in the simulations above some massive yields of fission thermal power have been seen.

If the sustained capture of mass in the shock tube core is a real effect then it bodes extremely well for the promise of the PMI-GCR class of pulsed fission reactors. One would have to ensure that some mechanism was in place for removing (pumping out) the significant concentration of compressed fuel in the reactor shock tube core to allow both cycling of the device as well as limiting damage due to the rapid increase in fission power.

It is hoped that once the magnetogasdynamic simulation code is modified to include the fission power source term and a better plasma kinetics model that some of the real gas effects will come into play to limit the compression effect without destroying the nonlinear shock interaction that produces the high fluid densities in the first place.

9.2   *Recommendations for Future Research*

The research findings reported above are strong results. They are however weakened by the lack of complete coupling of the nuclear and MHD codes. A full simulation of the shock generation and collision leading to fission energy release has therefore not been accomplished. Careful groundwork has, however, been laid that will make the completion of these unfinished tasks close to a formality with just one qualification: the need for gathering experimental data on high temperature UF_4 non-equilibrium partial plasma properties poses a nontrivial task.

There are three urgent tasks that are suggested as serious omissions that need to be carefully examined in any future research on this concept.

1. The fission source terms must be included in the MHD equation solver, and preferably 2-dimensional geometry should be modeled with viscous and heat conduction terms. Radiative losses should also be considered as the UF_4 partial plasma is likely to become optically very opaque during shock collision, but yet highly radiative due to the enormous combined effect of shock and fission heating that may raise the gas temperature up to millions of Kelvin.
2. UF_4 plasma thermoproperties and transport properties need to be modeled with more rigour. It is highly unsatisfactory to have the gas conductivity fixed at an arbitrary value somewhere between the equilibrium scalar conductivity of UF_4 and gas discharge conductivity. Experimental data is paramount for this effort. Experiments to measure UF_4 partial plasma conductivity and viscosity at high temperature are in urgent need to complement limited theoretical transport coefficient calculations.
3. The pulsed *B*-field shock generation mechanism was inadequately investigated. Although the MPD-compressor mode modeling also made gross approxi-mations such as zero current rise time and high ionization, the effectiveness of such a shock generation mechanism can be questioned and needs to be carefully evaluated before a huge amount of effort is put into costly experi-ments that might fail. Although pulsed high *B*-field shock generation is technically more demanding on the input power requirements, and also quite hazardous, nevertheless, it yet may prove to be the only way to generate strong shocks in UF_4 partial plasma. The reason is that the ambient UF_4 is nonconducting, or at least very weakly ionized (~1% ionization or lower) at ambient 2000^oK assumed for the reactor, so the entire effect of an MPD shock generator must depend upon gas discharge ionization, which is a local effect

and so does not ionize the gas between the shocks, only the shock fronts and the gas behind the incoming shocks will be ionized.

These tasks can be worked on separately to some extent, so there is ample reason to expect that a future phase of research can successfully address these concerns given only that sufficient human work hours are allocated. If the above tasks can be performed then simulations should be able to aid in the design of effective and worthwhile "zero power" shock tube experiments with non-fissile UF_4 (or with a chemically similar working fluid). This would be to validate shock generation and collision modeling, not fission power production. At a later stage of research, to simulate fission power production experimentally, a strong external heat source could be used to add thermal energy to the shock tube experiment as is found effective in conventional nuclear reactor testing programs that do not use actual fuel.

The analysis of the potential for power conversion has not been accomplished and waits for future research efforts. One needs to include the strong fission source terms in the MHD equations as mentioned above. Stronger post-collision shocks are expected to result when this effect is included, with potential for fairly efficient power conversion using the magneto-cumulative flux compression principle. For the power conversion stage at least one can say that the gas will be highly conducting due to the ionizing shock waves and fission product ionization. This will aid with fission-to-electric power conversion efficiency.

$$*\qquad*\qquad*$$

In summary, strong conclusions can be made on the overall feasibility of the PMI-GCR concept. There is no doubt that it can function as a viable power source. In some trials power densities of 10^{10} MeV.cm^{-3} are seen at the time of maximum density, and this can grow to 10^{30} MeV.cm^{-3} or even greater if the gas is left unperturbed in the center of the shock tube. This is a novel effect that was not predicted and has not been fully evaluated as a possible viable new means of fission power conversion. It is not yet fully known what regime of efficiency the system might operate at, or for what time periods, but the cycle time should be on the order of a few milliseconds. A limiting constraint might be how fast a capacitor bank can be recharged to start successive shocks, which has not been considered in this research. Strong recommendations are also made; especially one can single out fissioning partial plasma properties for UF_4 as urgently in need of *experimental* investigation.

A.1 ADDITIONAL SUBROUTINES FOR COUPLING THE MHD AND MCNP CODES

This subsection contains a brief description of the subroutines added to the MHD code. The script codes for MHD post-processing, MCNP preprocessing, MCNP post-processing, and MHD pre-processing will not be described here. The MCNP4C code is documented by Los Alamos National Laboratory and so is not described here either. So what remains is a brief description of the MHD code structure.

The main new subroutines added to the basic MHD code are,

SIM_STATUS: Determines whether the MHD simulation is continuing from a pause to run MCNP or starting fresh, opens data and log files for 'append' or 'new' access as appropriate.

MHDSAVE (ni,nf,filename): Used to store arrays for MHD1DSHOCK while MCNP is running.

MHDRETRIEVE (ni,nf,filename): Used to read back the array data saved by MHDSAVE once the script calls MHD1DSHOCK to resume a simulation.

MHDOUTPUT(ni,nf,ncols,fname): Writes data to a file 'mhdsout.dat' that can be read by the MCNP pre-processor, the data recorded includes cell coordinates and gas density at cell nodes, neutron source strength, neutron population from last time MCNP was called, and some data for MCNP input cards..

READMCNP (ni,nf,fname): Reads in coarse mesh cell coordinates, fission power density (="cqfiss" in the source code) q''' [MeV.cm^{-3} per neutron] (or specific power q[MeV/g per neutron]), and neutron flux (="cfluxn" in the source code) Φ_n [n.cm^{-2}.s^{-1} per neutron], and interpolates and extrapolates these values onto the fine MHD grid mesh (to arrays named "qfiss" and "fluxn" in the source code), scaling them by the neutron population scale factor "noft".

PLOTOUTPUT: Uses user supplied settings to record all data capturing the state of the fluid flow, magnetic field, and source terms. The user can specify one of two formats (e.g. Tecplot readable format, or a custom format) and can specify a certain time step interval between records by setting the variable "nframes", and can specify the number of cells of the grid to record data for by setting the variable "nxdata" (nxdata<nx is enforced, where nx=number of grid cells).

MHDSTOP(strstop): Halts the MHD1DSHOCK code with the correct return value to alert the script what appropriate action to take depending upon the value of the string "strstop".

A.1.1 New Input Parameters to the MHD Code

The original 'mhd1d.for' source code came with an include file 'mhdinc.inc' containing the common block variables, and a namelist file 'mhdin.dat' for entering the main simulation parameters such as the maximum time steps, the Courant number, the gas ratio γ (=1.07 for UF$_4$), and the plasma resistivity, ς [cm^2/s] (named "res" in the source code). To these files an extensive number of additional control variables, parameters and other structures have been added, so what was originally a 600 line F77 program called 'mhd1d.for' has been modified and extended into 5900 lines of F77 source code that has undergone three test version updates and is now called 'mhd1d_4.for'. It can be compiled using the GNU g77 FORTRAN to C compiler.

For a user the most important updates are the new variables and parameters in the new (version 4) namelist file 'mhdini.dat'. This is described next.

The contents of the input file 'mhdini.dat' consisting of 39 lines look at present as follows (default settings are somewhat arbitrary for some of these, but most are typical),

```
&run
nend=4000
nse=10
nsp=10
cr=0.4
ifluid=0
gamma=1.07
res=1.0E-10
nsg=10
leftbnd=0.0
sx=100.0
tperiod=1.0E-6
dtmcnp=1.0E-6
rhocrit=0.026
ncallmcnp=100
rhoin=0.0241
Pin=1.0E+7
bxi=1.0
byi=0.2E+3
nJzoff=0
ncurzon=500
physunits='cgs'
viewmhd='student'
nframes=145
nxdata=200
strlogfile='mhd1d.log'
```

```
strmcnpfile='mhdsout.dat'
strmhdinfile='mhdsin.dat'
strmhdsaved='mhdsaved.dat'
startfile='start.ini'
strmirrorfile='mirror.dat'
savedir='results/'
ncoremtrl=1
ncoreimp=1
source=1.0E+10
isfluxlim=F
isantidiff=F
ismcnp=T
isdebug=T
```

A brief synopsis these parameters and their functions are given in Appendix Table 7. The data types for each parameter are omitted here, but should be obvious.

Appendix Table 7. List of inputs to the MHD code, listing of namelist file 'mhdini.dat'.

nend	=	maximum number of timesteps (iterations) of the MHD solver.
nse	=	counter for the timestep at which a subset of the array data will be written to the file 'mhd1d.log'.
nsp	=	counter for the timestep in which output will be echoed to the screen terminal.
nsg	=	an additional (presently unused) counter.
cr	=	Default=0.4, the CFL number to satisfy the Courant-Friedrich-Levy condition.
ifluid	=	0, uses ideal gas equation of state to get T(P,rho)
	=	1, then uses user supplied empirical equation of state.
gamma	=	Gas ratio of specific heats.
res	=	Electrical resistivity of gas as a partial plasma, units $[cm^2.s^{-1}]$..
leftbnd	=	Default=0.0, axial coordinate (cm) of leftmost fluid cell left hand side boundary.
sx	=	Shock tube length, [cm].
tperiod	=	time period [secs] for calls to write array values to output files for later visualization of results.
dtmcnp	=	time increment [secs] at which to pause MHD program to call MCNP via the batch script.
rhocrit	=	minimum density required in the shock tube before the MHD code bothers invoking MCNP, i.e., for MCNP to be called some ro(j)>rhocrit is required.
ncallmcnp	=	option to specify maximum number of calls to MCNP during the simulation, e.g., if ncallmcnp=100 and there are nend=6000 time steps, then using ncallmcnp for control will pause to run MCNP every 60 time steps.
rhoin	=	initial density throughout tube [g/cc].
Pin	=	initial shock tube gas pressure [dynne/cm^2].
bxi	=	constant value of B_x/sqrt(4*pi) field. Units B_x:[gauss]
byi	=	boundary value for B_y/sqrt(4*pi) which sets the current J_z by setting the tangential components of the magnetic field intensity at the grid guard cells. (Very roughly by0(r,l) (-1.0,1.0) gives J_z=5.0E+12 [statamp/cm^2] (1,7E+7 [Amp/m^2]), for dx 0.166 cm, for other dx grid size J_z will be different because the exact value of J_z depends upon dx.)
nJzoff	=	0 to turn off boundary current when vx(nx/2) gets perturbed,

	=	1 to turn off boundary current after fixed time step.
ncurzon	=	A fixed integer time step after which the current at the boundary is turned off (in effect only when nJzoff=1) by resetting the boundary tangential magnetic field in the guard cells of the mesh to zero.
diff_tscale	=	The fraction by which to decrease the diffusion time scale dt_2. In the code this is, dt2=diff_tscale*dx*dx/res.
physunits	=	Option to specify whether using Gaussain (physunits='cgs') ro SI units (physunits='mks'), eg. one can use this to tell various functions whether to expect argument values in SI or cgs units and hence do necessary conversions. For example, some of the real gas thermoproperties are sometimes most conveniently entered in SI units, but the MHD source code proper employs Gaussian (cgs) units for computer integration of the governing equations.
viewmhd	=	type of visualization format to use when writing array data output for visualization. Presently must be either 'viewmhd', 'student' or 'tecplot'
nframes	=	desired number of time steps (out of a possible total=nend) for which array data will be recorded, ie.written to the visualization data files 'ro.dat', 'vx.dat', etc.,....
nxdata	=	maximum number of points (cell nodes) for which data will be written to 'ro.dat', vx.dat', etc...
strlogfile	=	specifies name of a log file that records diagnostic information about the simulation. The script does not care about this file.
strmcnpfile	=	Default='mhdsout.dat', the name of the file that the script program expects to see data from the MHD code relevant to the MCNP preprocessor script.
strmhdinfile	=	Default='mhdsin.dat', file that the script prepares containing results of MCNP output that will be read by the MHD code.
strmhdsaved	=	'mhdsaved.dat', contains all the arrays that the MHD code needs to remember for continuing the same simulation after temporarily halting to call MCNP. The script does not care about this file.
strstartfile	=	'start.ini', used to evaluate simulation status.
strmirrorfile	=	'mirror.dat', used for diagnosing bugs in retrieving data from MCNP and saved arrays from the file named by "strmhdsaved".
savedir	=	'results/', name of subdirectory to store simulation data output record files to.
ncoremtrl	=	constant used by MCNP preprocessor.
ncoreimp	=	constant used by MCNP preprocessor.
source	=	background neutron source parameter used by MCNP (neutrons/sec).
isfluxlim	=	logical constant , if isfluxlim=F, then flux limiting is turned off.
isantidiff	=	logical constant, if isantidiff=F, then antidiffusion step of FCT is turned off.
ismcnp	=	logical constant, ismcnp=T iff MCNP is to be used.
isdebug	=	If isdebug =F, then some lines of the log file output will be suppressed.

As one can see, most of the parameters are non-essential for the MHD solver algorithm in 'subroutine stepon', and the majority of the inputs are for controlling how MHD1D-SHOCK communicates with MCNP4C.

The main program loop and main additional subroutines will be listed next. The structure of the main program loop (mainly focusing on the program calls and control structures) is as follows in Appendix Table 8, for clarity subroutine calls and Fortran keywords are in blue, control structures are in red, ordinary assignment statements and so forth are in black, pseudocode is indicated in black between # marks, and comments are in plain text prefixed by exclamation marks.

Appendix Table 8. MHD1D_4.for Main Program Loop Structure.

Program MHD1D_ver4
issimgo=.false.   ! Initially assume that a new simulation case is to be run.
call input   ! Read inputs from namelist file 'mhdini.dat'.

call sim_status   ! Read the file 'start.ini' (named by the variable "strstartfile") to ascertain whether a
                  ! simulation is resuming after pausing to run MCNP, or if indeed a new simulation is
                  ! starting. 'start.ini' should contain a single record ="start" or ="continue" as appropriate.
                  ! A key task of this subroutine is to set the value of "issimgo" correctly.

if (.not.issimgo) then
    call initial   ! Set up initial conditions on the mesh only if starting a new job.
    #set fluxn(j) and qfiss(j) arrays to zero.#
    #initialize variables, e.g. nstep=0#
 end if

 # set integers for array maximums   ! Not all subroutines need the guard cells, so the min.and   **and minimums to be passed to var-**   ! max. index passed depends upon the task.   **ious subroutines, and set integers**   **controlling data output preferences.#**

if (issimgo) then
    call readmcnp( )   ! Get MCNP data if resuming a simulation.
    call mhdretrieve( )   ! Get saved MHD array data if resuming a simulation.
 end if

do while (nstep.le.nend)   ! Enter main MHD solver loop.
call setdt( )   ! Set the max allowable time step using the CFL condition.
call stepon( )   ! Transport the fluid and field variables one time step. This is the FCT algorithm.
#Perform some diagnostic checks   **e.g. save global maximum ρ,P,T#**
call bndry   ! Reset the boundary conditions as appropriate for new time step.
if (nstep.eq.1) cycle

if (#nstep or time is due for recording a frame of data#) then
       call plotoutput(nxskip)   ! Record arrays, but only every nxskip grid point.
    end if

#Check criteria for calling MCNP to   ! This sets the variables "isrhocrit" and "iscallmcnp".   **update fission power source terms#**

if (iscallmcnp) then
     delta=simtime-prevtime   ! This is the time since last call to MCNP, it is required by the
                      ! MCNP pre-processor.
     call mhdoutput(ni,nf,ncols,strmcnpfile)   ! Record data required by MCNP pre-processor.
     call mhdsave(ni,nf,strmhdsaved)   ! Save arrays and data required by MHD1DSHOCK to
                      ! restart from previous state when the script starts it again.
     call mhdstop('Pause')   ! Halt execution but return a value=1 to the OS that indicates
                  ! to the script that the simulation should continue after MCNP is done
                  ! updating the fission source terms.
    end if

end do
#Write a summary of simulation results   **to the log file and to the screen terminal.#**
call mhdstop('End')   ! Stop the simulation for good by sending return value=0 to the OS.
end

There are of course numerous other subroutines and user defined functions that are called by the main subroutines listed in the table, but it would be pedantic to describe them all here. The main critical background subroutine is "Coarse2FineInterp( )" that gets called twice by subroutine "readmcnp( )". Subroutine Coarse2FineInterp( ) takes array indices and array data (representing some function on a mesh) as arguments and interpolates data defined on a coarse mesh onto a finer mesh. In the MDH1DSHOCK code the coarse mesh array is read in from the MCNP results, while the fine mesh is just the MHD grid. Of all new procedures in the code this one is perhaps the least well tested and may still contain a few bugs. The subroutine "stepon( )" that integrates the MHD equations forward by one time step is the other procedure that can be improved, currently it operates best when flux-correction and anti-diffusion are turned off, and thus it operates as a leapfrog trapezoidal solver with strong artificial diffusion. This will not give unreasonable results for the reasonably high viscosity UF_4 gas fuel, but one should bear in mind that the equations being solved are not really physically accurate, although they are still qualitatively useful for suggesting future experiments and code modifications.

There are also additional user defined functions that can be used to compute the real gas properties as a function of temperature and pressure, however these are generally only valid for T=200 to 10 000°K, and for equilibrium UF_4 plasmas, so caution should be exercised in using them, and generally it was found that using ideal gas laws supplemented by a fixed electrical conductivity yielded acceptable results for the purposes of this study.

REPORT DOCUMENTATION PAGE

1. AGENCY USE ONLY *(Leave Blank)*	2. REPORT DATE May 2008	3. REPORT TYPE AND DATES COVERED Contractor Report

4. TITLE AND SUBTITLE

Gas Core Reactor Numerical Simulation Using a Coupled MHD-MCNP Model

5. FUNDING NUMBERS

NCC8–225

6. AUTHORS

F. Kazeminezhad and S. Anghaie

7. PERFORMING ORGANIZATION NAME(S) AND ADDRESS(ES)

Institute for Scientific Research, Inc.
320 Adams St.
P.O. Box 2720
Fairmont, WV 26555–2720

University of Florida
202 NSC
Gainesville, FL 32611–8300

8. PERFORMING ORGANIZATION REPORT NUMBER

M–1228

9. SPONSORING/MONITORING AGENCY NAME(S) AND ADDRESS(ES)

George C. Marshall Space Flight Center
Marshall Space Flight Center, AL 35812

10. SPONSORING/MONITORING AGENCY REPORT NUMBER

NASA/CR—2008–215408

11. SUPPLEMENTARY NOTES

Prepared for the Spacecraft and Vehicle Systems Department, Engineering Directorate
Technical Officer: Gary Johnson

12a. DISTRIBUTION/AVAILABILITY STATEMENT

Unclassified-Unlimited
Subject Category 20
Availability: NASA CASI 301–621–0390

12b. DISTRIBUTION CODE

13. ABSTRACT *(Maximum 200 words)*

Analysis is provided in this report of using two head-on magnetohydrodynamic (MHD) shocks to achieve supercritical nuclear fission in an axially elongated cylinder filled with UF4 gas as an energy source for deep space missions. The motivation for each aspect of the design is explained and supported by theory and numerical simulations. A subsequent report will provide detail on relevant experimental work to validate the concept. Here the focus is on the theory of and simulations for the proposed gas core reactor conceptual design from the onset of shock generations to the supercritical state achieved when the shocks collide. The MHD model is coupled to a standard nuclear code (MCNP) to observe the neutron flux and fission power attributed to the supercritical state brought about by the shock collisions. Throughout the modeling, realistic parameters are used for the initial ambient gaseous state and currents to ensure a resulting supercritical state upon shock collisions.

14. SUBJECT TERMS

propulsion, power, nuclear, gas core reactor, magnetohydrodynamics (MHD), colliding shocks

15. NUMBER OF PAGES

78

16. PRICE CODE

17. SECURITY CLASSIFICATION OF REPORT Unclassified	18. SECURITY CLASSIFICATION OF THIS PAGE Unclassified	19. SECURITY CLASSIFICATION OF ABSTRACT Unclassified	20. LIMITATION OF ABSTRACT Unlimited

National Aeronautics and
Space Administration
IS20
George C. Marshall Space Flight Center
Marshall Space Flight Center, Alabama
35812